iScience

CellPress
OPEN ACCESS

Article

Membrane HIV-1 envelope glycoproteins stabilized more strongly in a pretriggered conformation than natural virus Envs

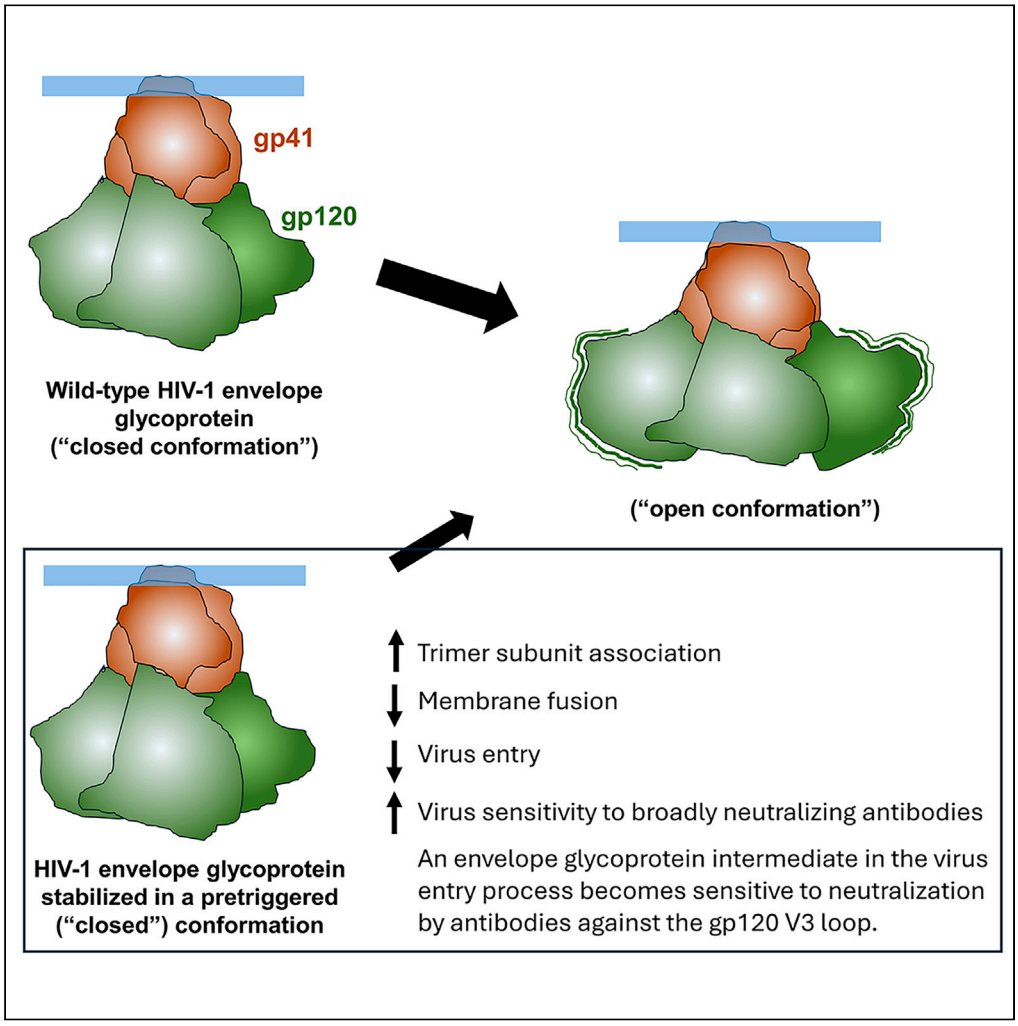

Zhiqing Zhang, Saumya Anang, Hanh T. Nguyen, Christopher Fritschi, Amos B. Smith III, Joseph G. Sodroski

joseph_sodroski@dfci.harvard.edu

Highlights

Envs from diverse HIV-1 clades can be stabilized in the pretriggered conformation

Stabilized envelope glycoproteins fuse membranes and enter cells slowly

Most broadly neutralizing antibodies recognize stabilized envelope proteins better

V3 poorly neutralizing antibodies neutralize highly stabilized Env intermediates

Zhang et al., iScience 27, 110141
July 19, 2024
https://doi.org/10.1016/j.isci.2024.110141

iScience

CellPress
OPEN ACCESS

Article

Membrane HIV-1 envelope glycoproteins stabilized more strongly in a pretriggered conformation than natural virus Envs

Zhiqing Zhang,[1,2,4] Saumya Anang,[1,2,4] Hanh T. Nguyen,[1,2] Christopher Fritschi,[3] Amos B. Smith III,[3] and Joseph G. Sodroski[1,2,5,*]

SUMMARY

The pretriggered conformation of the human immunodeficiency virus (HIV-1) envelope glycoprotein (Env) trimer ((gp120/gp41)$_3$) is targeted by virus entry inhibitors and broadly neutralizing antibodies (bNAbs). The lability of pretriggered Env has hindered its characterization. Here, we produce membrane Env variants progressively stabilized in pretriggered conformations, in some cases to a degree beyond that found in natural HIV-1 strains. Pretriggered Env stability correlated with stronger trimer subunit association, increased virus sensitivity to bNAb neutralization, and decreased capacity to mediate cell-cell fusion and virus entry. For some highly stabilized Env mutants, after virus-host cell engagement, the normally inaccessible gp120 V3 region on an Env intermediate became targetable by otherwise poorly neutralizing antibodies. Thus, evolutionary pressure on HIV-1 Env to maintain trimer integrity, responsiveness to the CD4 receptor, and resistance to antibodies modulates pretriggered Env stability. The strongly stabilized pretriggered membrane Envs reported here will facilitate further characterization of this functionally important conformation.

INTRODUCTION

The entry of human immunodeficiency virus (HIV-1) into host cells is mediated by the envelope glycoprotein (Env) trimer ((gp120/gp41)$_3$) on the surface of the viral membrane.[1,2] In HIV-1-infected cells, the gp160 Env precursor is modified by glycans, cleaved to produce the noncovalently associated gp120 exterior envelope glycoprotein and gp41 transmembrane glycoprotein, and incorporated into virions.[3–9] During virus entry, gp120 binds the host cell receptors, CD4 and CCR5/CXCR4.[10–15] CD4 binding drives the metastable Env from a "closed," pretriggered conformation through a default intermediate conformation to an "open," CD4-bound prehairpin intermediate.[16–18] Binding of the prehairpin intermediate to the CCR5 or CXCR4 coreceptor results in the formation of a highly stable gp41 six-helix bundle, which promotes the fusion of the viral and cell membranes.[19–21]

Small-molecule inhibitors can block HIV-1 entry by initially interacting with the pretriggered Env and modulating Env conformation. BMS-806 analogs stabilize the pretriggered conformation and prevent transitions to downstream conformations necessary for virus entry.[16,22,23] By contrast, CD4-mimetic compounds (CD4mcs) compete with CD4 and also trigger conformational changes in Env similar to those induced by CD4, driving the pretriggered Env into more open downstream conformations.[16,24–27] In the immediate vicinity of a target membrane expressing CCR5, these CD4mc-induced Env intermediates can support virus entry; however, the activated intermediates are short-lived and, in the absence of an appropriate target membrane, undergo irreversible inactivation.[25,28,29] Changes in the stability of the pretriggered Env conformation alter HIV-1 susceptibility to CD4mc inhibition and are thought to contribute to the wide range of sensitivities of naturally occurring HIV-1 strains to these compounds.[17,27,30–33] The propensity of HIV-1 Env variants to undergo conformational transitions from the pretriggered state has been termed triggerability or reactivity and is inversely related to the activation energy barriers separating this state from downstream conformations.[17,31]

As the only virus-specific molecule on the virion surface, Env is a major target for host antibodies. Env's heavy glycosylation, strain-dependent sequence variability, conformational flexibility, and structural lability are thought to contribute to the ability of HIV-1 to evade the host antibody response.[1,34–37] During natural infection, high titers of antibodies are elicited that recognize the conformationally flexible gp160 Env precursor and disassembled Envs (shed gp120, gp41 six-helix bundles).[35,36,38–40] These antibodies are poorly neutralizing (pNAbs) because they fail to recognize the mature functional Env trimer, which mainly resides in a pretriggered conformation.[16,41–44] After several years of

[1]Department of Cancer Immunology and Virology, Dana-Farber Cancer Institute, Boston, MA 02215, USA
[2]Department of Microbiology, Harvard Medical School, Boston, MA 02115, USA
[3]Department of Chemistry, University of Pennsylvania, Philadelphia, PA 19104, USA
[4]These authors contributed equally
[5]Lead contact
*Correspondence: joseph_sodroski@dfci.harvard.edu
https://doi.org/10.1016/j.isci.2024.110141

infection, broadly neutralizing antibodies (bNAbs), most of which recognize the pretriggered Env conformation, are elicited in some HIV-1-infected individuals.[16,35,44–49] Passively administered monoclonal bNAbs are protective in animal models of HIV-1 infection, suggesting that the elicitation of bNAbs is an important goal for vaccines.[50–53] Unfortunately, bNAbs have not been efficiently and consistently elicited in animals immunized with current Env vaccine candidates, including stabilized soluble gp140 (sgp140) SOSIP.664 trimers.[54–59]

Structural studies indicate that bNAbs need either to bypass the HIV-1 Env glycan shield to engage conserved protein surfaces (e.g., the gp120 CD4-binding site and the gp41 membrane-proximal external region [MPER]) or to bind Env epitopes consisting at least partly of glycans.[37,60–69] In either case, bNAbs need to engage the functional Env trimer on the viral membrane at precise angles of approach[62–70]; bNAbs undergo extensive evolution from their germline precursors to do so.[35,66,67,69,71–78] During natural HIV-1 infection, the evolution of most bNAbs likely is driven by the mature pretriggered Env trimer on the virus or cell membrane. The association of Env with the membrane is important for maintaining a pretriggered conformation and for the correct composition of Env glycans, both of which can influence the binding of bNAbs and their precursors.[79–89] However, even the mature membrane-anchored Env trimer exhibits some flexibility, with individual protomers sampling more open conformations.[16,90] These conformationally dynamic Env trimers may divert the evolution of potentially neutralizing antibodies that need to engage pretriggered Env trimers at precise angles of approach.[62–70,89] More open Env trimers are also more prone to gp120 shedding and loss of structural integrity, thus exposing many immunodominant epitopes not accessible on the functional pretriggered Env.[23,28,29,90,91]

Multiple immunogenicity studies in animals indicate that stabilized sgp140 SOSIP.664 Env trimers elicit strain-specific neutralizing antibodies and pNAbs but not bNAbs.[54–59] Differences in the antigenicity, glycosylation, and conformation of sgp140 SOSIP.664 trimers and functional membrane Envs have been observed.[80,81,92–97] Given the importance of the functional HIV-1 membrane Env as a target for entry inhibitors and as a potential vaccine immunogen, characterizing the structure and evaluating the immunogenicity of the pretriggered Env conformation represent high priorities. Achieving these objectives would be facilitated by having membrane Envs that are exclusively or predominantly in a pretriggered conformation. Structural information on the pretriggered membrane Env conformation that is sufficiently detailed to guide such efforts is currently lacking. Moreover, Env changes that stabilize sgp140 SOSIP.664 trimers do not necessarily stabilize the pretriggered conformation of membrane Envs.[97–114] Conversely, several changes that have been found to stabilize the pretriggered conformation of membrane HIV-1 Envs involve Env regions that are heterogeneous or disordered in sgp140 SOSIP.664 trimer structures.[32,33,109,110,113,114] For these reasons, efforts to stabilize the pretriggered conformation of membrane Envs have proceeded empirically. In that process, we have identified several natural Env amino acid polymorphisms that individually stabilize the pretriggered conformation of the functional HIV-1 membrane Env trimer.[32,33,110,115] Here, we demonstrate that combinations of these changes yield Env variants from diverse HIV-1 strains that are additively stabilized in a pretriggered conformation, some to a degree well beyond that of natural HIV-1 strains. Increased stability of the pretriggered Env conformation correlated with increased trimer subunit association, increased sensitivity to neutralization by conformation-dependent bNAbs, and decreased capacity to mediate membrane fusion and virus entry. Functional intermediates of the most stabilized Env mutants exhibited increased sensitivity to neutralization by pNAbs directed against the gp120 V3 region and bNAbs against the gp41 MPER, but only after engagement of the target cell by the virus. These studies provide valuable insights into the evolutionary advantages and liabilities of HIV-1 modulating the stability of the pretriggered Env conformation. The strongly stabilized membrane Env variants reported herein will facilitate further characterization of this functionally important state.

RESULTS

Phenotypes of stabilized pretriggered HIV-1 Envs

Compared with their unstabilized Env counterparts, viruses with functional HIV-1 Envs that are stabilized in a pretriggered conformation exhibit relative resistance to soluble CD4 (sCD4), CD4mcs, and exposure to cold (0°C).[32,33,87,90,91,110] By screening natural Env polymorphisms, we identified several that conferred phenotypes associated with stabilization of the pretriggered HIV-1_{AD8} Env.[32,110,115] We also identified two examples where combinations of individual Env changes enhanced these phenotypes in an additive manner: (1) a set of three changes (Q114E/Q567K/A582T) (herein called Tri) involving interior gp120 and gp41 elements near the trimer axis[32] and (2) a set of three changes (A532V/I535M/L543Q) in the gp41 fusion peptide-proximal region (herein called FPPR)[110] (Figure S1). To evaluate the potential additivity of the Tri and FPPR modifications as well as other Env changes (K59A, H66N, N136E, N136Q, T138A, V255I, A316W, D325Q, R440A, and K574R) individually implicated in stabilization of the pretriggered Env,[32,33,58,91,110,111] we made and analyzed HIV-1_{AD8} Envs with multiple combinations of these changes (Figure S1). The mutant Envs were evaluated for processing, subunit association, gp120 association with detergent-solubilized trimers, and ability to mediate cell-cell fusion and pseudovirus infectivity (Figure 1). The sensitivity of recombinant viruses pseudotyped with the Env variants to inhibition by CD4mcs and cold inactivation was also assessed (Figure 2A). Envs that exhibited efficient processing and subunit association and were relatively resistant to CD4mcs and cold were given priority for additional analysis. The mutant Envs in this panel were proteolytically processed at least as efficiently and, in most cases, more efficiently than the wild-type (wt) HIV-1_{AD8} Env (Figure 1). The integrity of the Env trimer, reflected in the measured level of association between the gp120 and gp41 subunits, was enhanced as the number of introduced Env modifications increased. Decreases in the ability of Env to mediate cell-cell fusion and virus infection also accompanied the increase in the number of introduced Env changes. As expected for Envs with potential decreases in triggerability, the viruses pseudotyped with the Tri FPPR and Tri FPPR variant Envs were markedly resistant to inhibition by the indane CD4mc, BNM-III-170, and cold inactivation at 0°C (Figure 2A). For example, compared with the parental wt AD8 virus, the Tri FPPR virus was 56-fold more resistant to BNM-III-170 and 23-fold more resistant to cold inactivation. Based on these phenotypes, several of the Tri FPPR Env derivatives in Figure 2A

Env	Processing	Subunit association	gp120-trimer association	Cell-cell fusion (%)	Infectivity (%)
wt AD8	1	1	1	100	100
Tri	3.25 ± 0.36	2.91 ± 0.61	1.07 ± 0.06	55.0 ± 13.0	79.0 ± 18.0
FPPR	1.69 ± 0.19	1.99 ± 0.41	1.15 ± 0.06	56.9 ± 21.5	48.0 ± 16.0
Tri FPPR	8.24 ± 0.92	2.68 ± 0.56	0.43 ± 0.02	71.0 ± 7.84	17.0 ± 7.14
Tri FPPR-K59A	4.11 ± 0.46	3.88 ± 0.81	1.44 ± 0.08	60.8 ± 11.8	9.76 ± 2.20
Tri FPPR-H66N	4.88 ± 0.55	2.30 ± 0.48	1.36 ± 0.07	7.00 ± 2.00	< 1
Tri FPPR-N136Q	3.73 ± 0.02	4.52 ± 0.40	0.87 ± 0.05	72.0 ± 13.0	11.0 ± 2.00
Tri FPPR-N136E	8.30 ± 0.93	4.34 ± 0.90	1.36 ± 0.07	67.1 ± 20.1	16.7 ± 6.92
Tri FPPR-T138A	3.30 ± 0.02	4.75 ± 0.42	1.22 ± 0.07	82.0 ± 15.0	7.00 ± 1.00
Tri FPPR-A316W	ND	ND	ND	50.5 ± 1.21	5.73 ± 0.67
Tri FPPR-K574R	4.66 ± 0.52	4.68 ± 0.97	1.25 ± 0.07	40.8 ± 12.7	10.1 ± 5.15
Tri FPPR-K59A/N136E	2.50 ± 0.02	5.01 ± 0.44	1.39 ± 0.08	26.0 ± 5.70	3.00 ± 0.00
Tri FPPR-K59A/T138A	2.57 ± 0.02	3.75 ± 0.33	1.54 ± 0.09	34.0 ± 9.00	1.00 ± 0.00
Tri FPPR-K59A/K574R	4.20 ± 0.17	5.27 ± 0.62	0.64 ± 0.14	14.5 ± 1.94	1.06 ± 0.08
Tri FPPR-N136E/K574R	4.23 ± 0.17	8.22 ± 0.97	0.78 ± 0.17	25.8 ± 3.78	3.00 ± 1.00
Tri FPPR-A316W/K574R	ND	ND	ND	13.3 ± 0.96	1.18 ± 0.13
Tri FPPR-K59A/N136E/K574R	3.72 ± 0.15	9.32 ± 1.10	0.46 ± 0.10	4.61 ± 0.59	< 1
Tri FPPR-K59A/A316W/K574R	ND	ND	ND	3.46 ± 0.50	< 1

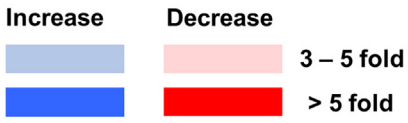

Figure 1. Phenotypes of HIV-1_{AD8} Env variants

Env processing, subunit association, gp120-trimer association, and ability to mediate cell-cell fusion and virus infectivity are shown for the wt and variant HIV-1_{AD8} Envs, normalized to those values observed for the wt HIV-1_{AD8} Env. Values are colored according to the key, based on their fold increase or decrease compared with those of the wt HIV-1_{AD8} Env. The results shown are the means and standard deviations derived from at least two independent experiments. See also Table S1 and Figures S1–S3.

are strong candidates for stabilized pretriggered Envs. Conversely, some combinations of Env changes failed to improve the desired phenotypes and were assigned a lower priority for further study (Table S1).

Using virus sensitivity to CD4mcs and cold as surrogates of Env triggerability, we sought to evaluate quantitatively the potential benefit of introducing additional changes in the Tri FPPR Env. However, the magnitude of resistance of the Tri FPPR virus to BNM-III-170 and cold made ranking the relative contributions of the additional Env changes difficult. Therefore, we measured the sensitivity of viruses pseudotyped with the Env variants to CJF-III-288, a recently discovered indoline CD4mc that inhibits HIV-1 infection more potently than BNM-III-170.[27] The higher potency of CJF-III-288 allowed us to determine IC_{50} values for most of the Env variants (Figure 2A). We used the product of the CJF-III-288 IC_{50} and the half-life of virus infectivity at 0°C to calculate a pretriggered Env stability index, providing a quantitative means to rank the relative triggerability of the Env variants.[32,33,87,90,91,110,111] Tri FPPR-K574R Env variants with one or more additional changes (K59A, N136E, or A316W) exhibited the highest pretriggered Env stability indices. By these criteria, the stabilities of the pretriggered

A

Env	CD4mc sensitivity IC_{50} (μM)		Cold ($t_{1/2}$) (days)	$t_{1/2}$ (days) (CD4mc + cold)	
	BNM-III-170	CJF-III-288		BNM-III-170 (100 μM)	CJF-III-288 (10 μM)
wt AD8	2.30 ± 0.50	0.40 ± 0.02	0.59 ± 0.05	<0.04	<0.04
Tri FPPR	129.7 ± 7.50	12.4 ± 2.50	> 19	2.10 ± 0.90	0.55 ± 0.37
Tri FPPR-K59A	> 200	75.0 ± 8.50	> 19	0.91 ± 0.05	0.33 ± 0.13
Tri FPPR-N136Q	> 200	79.7 ± 8.50	17.8 ± 1.10	1.53 ± 0.80	0.69 ± 0.27
Tri FPPR-N136E	> 200	83.3 ± 7.30	> 19	3.29 ± 0.90	0.96 ± 0.08
Tri FPPR-T138A	> 200	69.8 ± 4.50	> 19	2.07 ± 0.12	0.48 ± 0.04
Tri FPPR-A316W	> 200	83.0 ± 9.62	> 19	ND	1.40 ± 0.42
Tri FPPR-K574R	> 200	86.8 ± 7.50	19	16.7 ± 2.50	6.22 ± 2.14
Tri FPPR-K59A/N136E	> 200	169.8 ± 16.9	16.1 ± 2.50	2.12 ± 0.50	0.88 ± 0.16
Tri FPPR-K59A/T138A	> 200	162.2 ± 19.2	> 19	1.44 ± 0.70	0.93 ± 0.42
Tri FPPR-K59A/K574R	> 200	167.3 ± 17.6	> 19	> 19	18.5 ± 2.12
Tri FPPR-N136E/K574R	> 200	161.5 ± 21.6	> 19	> 19	9.26 ± 3.87
Tri FPPR-A316W/K574R	> 200	> 200	18	ND	8.70 ± 2.55
Tri FPPR-K59A/N136E/K574R	> 200	> 200	> 19	> 19	14.4 ± 5.55
Tri FPPR-K59A/A316W/K574R	> 200	> 200	> 19	ND	8.61 ± 3.27

IC_{50} (μM)	0-50	50-100	100-200
Days	< 1	1-10	> 10

B

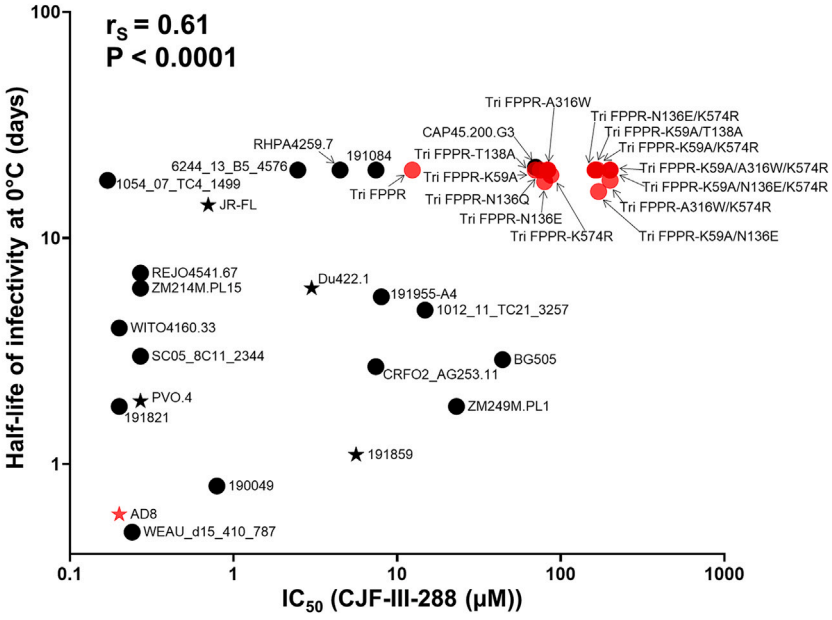

Figure 2. Effects of CD4-mimetic compounds and cold exposure on the infectivity of HIV-1_{AD8} Env variants and primary HIV-1 strains

(A) The 50% inhibitory concentration values (IC_{50} values) of the CD4-mimetic compounds (CD4mcs), BNM-III-170 and CJF-III-288, are reported in μM. Cold sensitivity is reported as the half-life (in days) of the infectivity of pseudotyped viruses incubated on ice. In the CD4mc+cold inhibition assay, 100 μM BNM-III-170 or 10 μM CJF-III-288 was incubated with the pseudotyped viruses for 1 h at 37°C. The CD4mc-virus mixtures were then incubated on ice for various lengths of time and used to infect Cf2Th-CD4/CCR5 cells. The half-lives (in days) of infectivity of the viruses are shown. The infectivity of viruses with the wt HIV-1_{AD8} Env was reduced to near-background levels by incubation with the CD4mcs for 1 h at 37°C. The results shown are the means and standard deviations derived from at least two independent experiments. Values are colored according to the key.

(B) For viruses pseudotyped with the indicated Envs, the half-life (in days) of the infectivity of viruses after incubation on ice is plotted against the CJF-III-288 IC_{50} (μM) on a log-log scale. The parental primary HIV-1 strains used to generate the stabilized Envs in this study are designated with stars. The wt HIV-1_{AD8} Env (red star) and the HIV-1_{AD8} Env mutants stabilized in a pretriggered state (red dots) are shown. In this plot, the upper-right quadrant is populated by the Env variants with greater stability of the pretriggered state (i.e., lower Env triggerability). Note that most of the stabilized HIV-1_{AD8} Env mutants (red dots) exhibit phenotypes associated with pretriggered Env stability that exceed those of a panel of representative diverse primary HIV-1 strains (black dots and black/red stars). See also Tables S1 and S2 and Figures S2 and S3.

conformation of these HIV-1_{AD8} Env derivatives are well beyond those found in the vast majority of Envs from diverse primary HIV-1 strains (Figure 2B; Table S2).

As a second approach to monitor HIV-1 Env triggerability, we utilized an assay in which the pseudotyped viruses were first exposed to a high concentration of either BNM-III-170 or CJF-III-288 at 37°C for 1 h and then incubated on ice in the continuous presence of the CD4mc for up to 19 days. The half-life of virus infectivity was determined. For comparison with other stabilized HIV-1_{AD8} membrane Env trimers, we evaluated the Comb G mutant (I535M/L543Q/K574R).[96,113,114] In this more stringent assay, the infectivity of the wt AD8 virus was completely eliminated after the 1-h exposure to these high concentrations of BNM-III-170 or CJF-III-288 (Figures 2A and S2A–S2D). The Comb G mutant was more stable, retaining 90% of its infectivity after a 1-h incubation with BNM-III-170 but only 10% of its infectivity following an additional 24-h incubation on ice (Figure S2D). Representative primary Tier-2 and Tier-3 neutralization-resistant viruses (JR-FL and PV0.4, respectively) likewise retained less than 15% of their initial infectivity after 24 h in this assay. By comparison, after 72 h of exposure to BNM-III-170 and 0°C, the virus with the Tri FPPR-K574R Env retained ~75% of its initial infectivity. Notably, the infectivity of the Tri FPPR-K59A/K574R, Tri FPPR-N136E/K574R, and Tri FPPR-K59A/N136E/K574R viruses in this assay was minimally affected even after 19 days of incubation on ice! The results with CJF-III-288 were consistent with those obtained using BNM-III-170 (Figures 2A, S2B, and S2D). Thus, these more stringent assays provided quantitative data on the relative resistance of the Env mutants to CD4mc and cold, phenotypes strongly associated with stabilization of the pretriggered conformation.[32,33,87,90,91,110,111]

Compared with the wt AD8 virus, viruses pseudotyped with the Tri FPPR Env variants exhibited greatly diminished activation of infection of CD4-negative, CCR5-expressing cells in response to the CD4mcs (Figure S3A), consistent with their lower triggerability.

CD4mc- and cold-induced gp120 shedding from Envs on virus particles

We recently reported that, by analyzing the antigenicity and CD4mc/cold-induced shedding of gp120 from virus particles, Envs with different levels of triggerability could be distinguished.[90] Importantly, even Envs with diminished function in supporting virus entry can be evaluated in these assays.[90] Studies of virus particles produced by pNL4-3.env infectious molecular proviral clones were conducted using Envs with Bam changes (S752F/I756F), which minimize clipping of the gp41 cytoplasmic tail by the HIV-1 protease but do not affect Env antigenicity or sensitivity to antibody neutralization.[90]

First, we examined the effects of Tri, FPPR, and additional (K59A, H66N, N136E, A316W, and K574R) changes on Env processing and incorporation into virus particles. Env processing and the levels of mature Env in virus particles were at least as great as those of the Tri FPPR Bam Env for most of the Tri FPPR Bam variants with additional changes (Figure 3A, summarized in Figure 3C). The levels of cleaved Env were slightly increased for some of the Tri FPPR Bam variants with combinations of additional changes.

Next, we examined gp120 shedding from virus particles in the presence of the CD4mc BNM-III-170 after incubation at room temperature for 1 h or at 0°C for one or two days. Shedding of gp120 from the Tri Bam Env was readily detected under all three conditions (Figure 3B), consistent with the results of our previous study.[90] The Tri FPPR Bam Env was much more resistant to gp120 shedding under these conditions; the addition of the FPPR changes to the Tri Bam Env reduced gp120 shedding by ~5-fold following a 1-day incubation on ice (Figure 3C, right column). Compared with the Tri FPPR Bam Env, the Tri FPPR Bam variants with individual additional changes (K59A, H66N, N136E, A316W, or K574R) were slightly more resistant to gp120 shedding, with K574R exerting the largest (~3.9-fold) effect. The three Tri FPPR Bam Envs with K574R combined with K59A, N136E, or both changes exhibited the most resistance to CD4mc+cold exposure, with 6.5- to 9.8-fold reductions in gp120 shedding compared with that of the Tri FPPR Bam Env (Figures 3C and 3D). The Tri FPPR Bam-K59A/K574R Env was ~40 times more resistant to gp120 shedding in response to CD4mc+cold exposure than the Tri Bam Env, which in turn is significantly more resistant to CD4mc and cold than the wt AD8 Env.[90] For this panel of HIV-1_{AD8} Env mutants progressively stabilized in a pretriggered state, CD4mc/cold-induced gp120 shedding from the virus Env trimers correlated with inactivation of the functional Env spike (Spearman $r_S = 0.949$, $p < 0.05$) (Figure 4A).

Relationship of pretriggered Env stability to other HIV-1 phenotypes

We examined potential correlations between the stability of the pretriggered HIV-1_{AD8} Env conformation and other HIV-1 phenotypes. Not surprisingly, the pretriggered Env stability index positively correlated with the infectious half-life of the pseudoviruses exposed to a combination of CJF-III-288 and cold ($r_S = 0.849$, $p = 0.0001$) (Table S3). We found that either the pretriggered Env stability index or the CD4mc+cold half-life could be used to evaluate the relationship between the stability of the pretriggered state and other Env phenotypes with nearly equivalent results (Table S3). These indicators of pretriggered Env stability correlated inversely with the amount of gp120 shed following exposure of virion Envs to a combination of CD4mc and 0°C (Figure 4B; Table S3). Both pretriggered Env stability indices correlated positively with subunit association of the Env mutants but not with gp120-trimer association (Figure 4C; Table S3). Subunit association monitors Env trimer stability in a native cell membrane environment, whereas gp120-trimer association measures the stability of the Env trimers extracted from membranes by solubilization in detergent, a process that can disrupt the pretriggered state.[39,88,89] The efficiencies with which the HIV-1_{AD8} Env mutants mediated cell-cell fusion and virus infection were negatively correlated with indicators of pretriggered Env stability (Figures 4D and 4E; Table S3). Target cell levels of CD4 apparently influence the infectivity of this panel of HIV-1_{AD8} Env mutants, based on the sensitivity of virus infection to the SIM.2 monoclonal antibody against CD4 (Figure 4F). No significant relationship between the indicators of Env triggerability and inhibition by maraviroc, a CCR5 inhibitor,[116] was seen (Tables S3 and S4). Thus, stabilization of the pretriggered HIV-1_{AD8} Env is accompanied by tighter association of the gp120 and gp41 subunits, less responsiveness to triggering by CD4 and CD4mcs, and a decrease in membrane-fusing and virus entry functions.

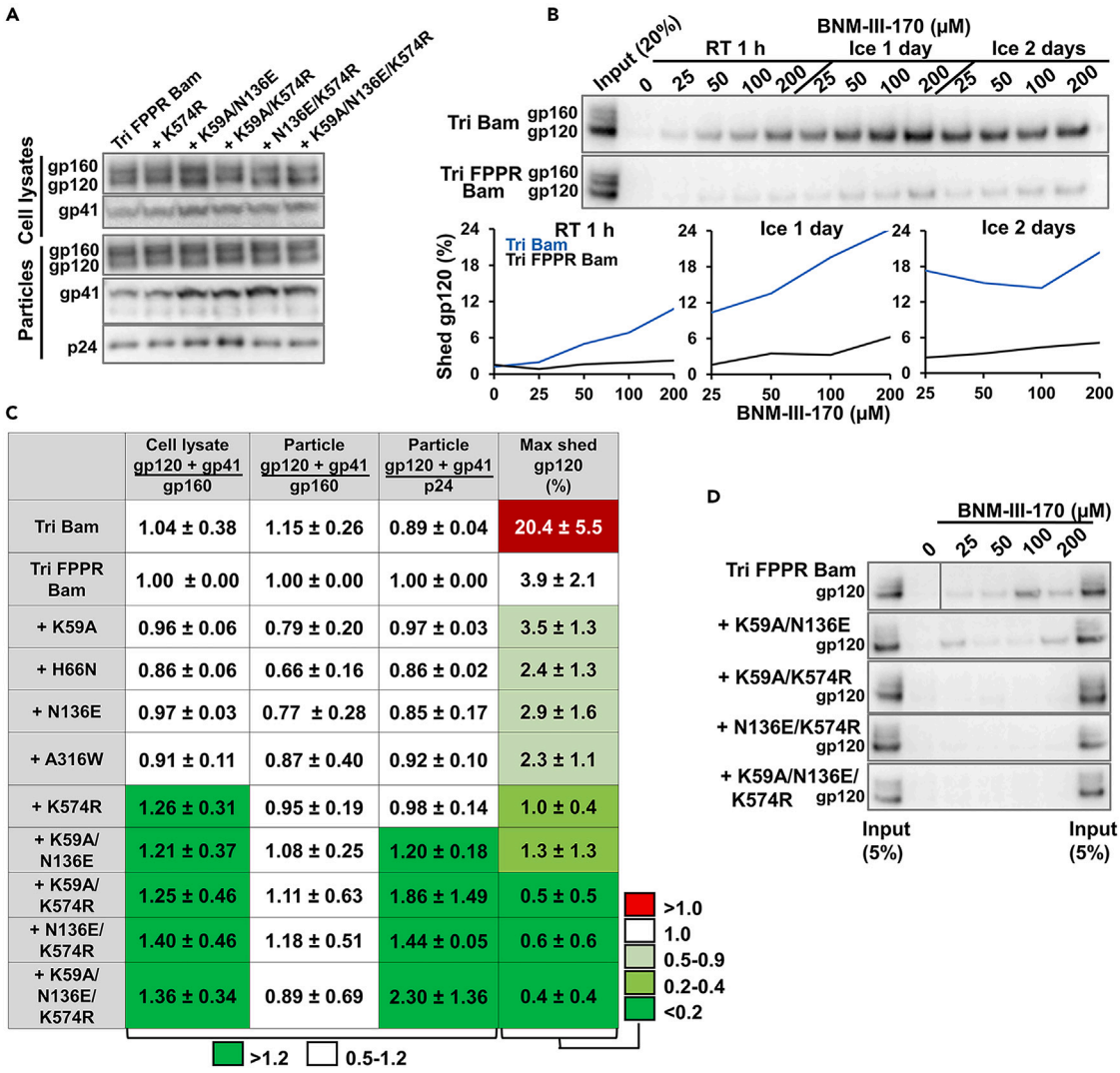

Figure 3. Processing, virion incorporation, and gp120 shedding of Tri FPPR Bam Env variants

(A) HEK293T cells were transfected with the pNL4-3.AD8 Bam plasmid containing an infectious HIV-1 provirus with the indicated changes in HIV-1_{AD8} Env. "Bam" indicates the presence of S752F/I756F changes in the Env cytoplasmic tail that prevent gp41 clipping by the HIV-1 protease in the virus particles.[90] Virus particles pelleted at 14,000 × g from cell supernatants and clarified cell lysates were western blotted with a goat anti-gp120 antibody, the 4E10 anti-gp41 antibody, and mouse anti-$p24^{CA}$ serum.

(B) Tri Bam and Tri FPPR Bam virus particles, purified as described in (A) but at 100,000 x g, were resuspended in 1× PBS and incubated with BNM-III-170 at the indicated concentrations, for 1 h at room temperature (RT) or 1 or 2 days on ice. Virus particles were then pelleted and the shed gp120 in the supernatants was captured with Galanthus nivalis lectin (GNL) beads and western blotted with a goat anti-gp120 antibody. The percentage of shed gp120 Env relative to the input gp120 on the virus particles is plotted in the graphs.

(C) Levels of processing and virion incorporation of Tri Bam Env and Tri FPPR Bam Env mutants are reported. The maximum percentage of gp120 shed after incubation of the virions with 200 μM BNM-III-170 at 0°C for one day is reported in the column on the right. Values are colored according to their fold change relative to those of the Tri FPPR Bam virus. Desirable phenotypes (i.e., an increase in cleaved Env or a reduction in gp120 shedding) are colored green. The results are representative of those obtained in at least two independent experiments, with means and standard deviations reported.

(D) Shedding of gp120 from virus particles with Tri FPPR Bam Env and Tri FPPR Bam Env mutants after a 1-day incubation on ice with the indicated concentrations of BNM-III-170 was analyzed as described in (B). See also Figure S4.

Antigenic profile of Envs on virus particles

We studied the antigenicity of the HIV-1_{AD8} Env variants on virus particles. We showed previously that Envs like Tri Bam that are stabilized in a pretriggered conformation differ antigenically from the wt AD8 Bam Env; i.e., Tri Bam gp120 was recognized less efficiently by pNAbs like the 19b anti-V3 antibody and the CD4-induced (CD4i) antibodies 17b and E51.[90] To examine how FPPR changes affect Tri Bam Env antigenicity, we compared the recognition of Tri Bam and Tri FPPR Bam Envs by a panel of bNAbs and pNAbs. As seen in Figure S4A, no significant

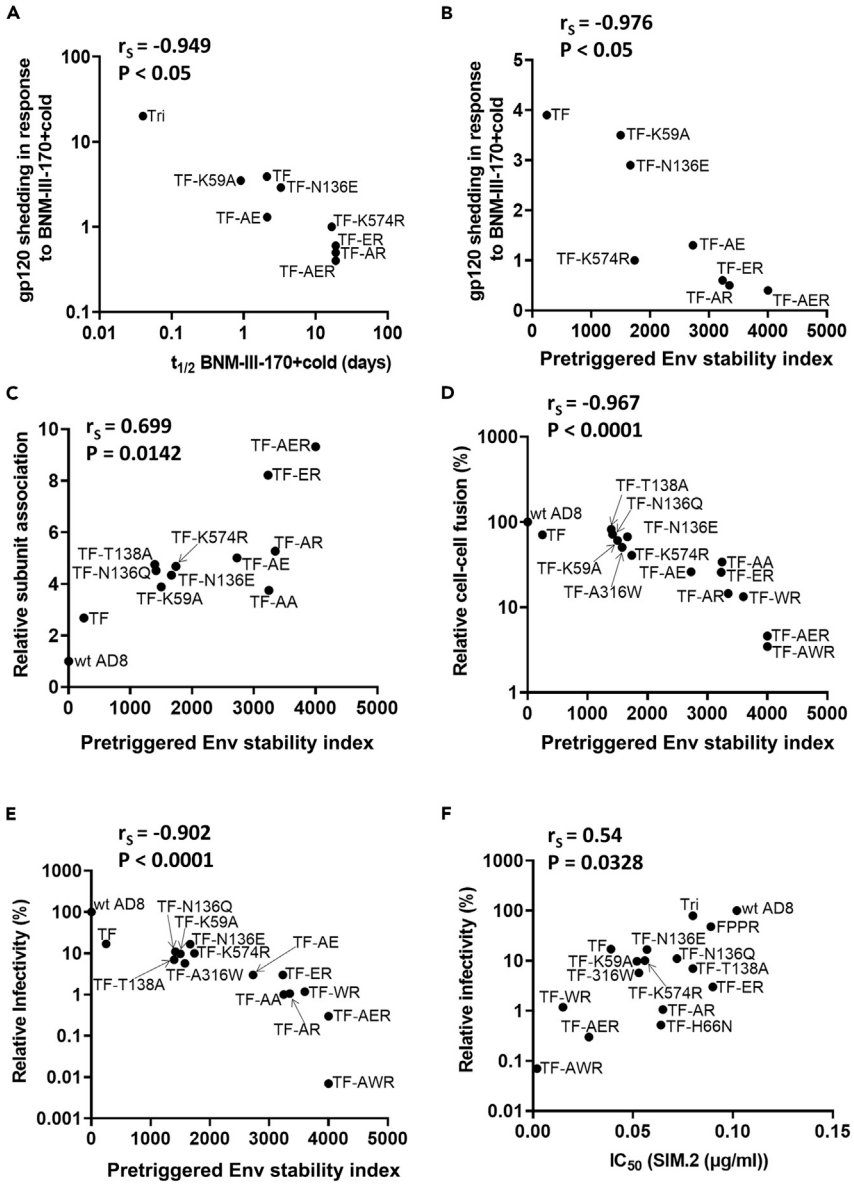

Figure 4. Relationship of pretriggered Env stability to other HIV-1 properties

(A) The relationship is shown between the infectious half-life ($t_{1/2}$) of viruses pseudotyped with the indicated Envs and gp120 shedding from the virus particles following exposure to 100 µM BNM-III-170 + cold (0°C).

(B–E) The pretriggered Env stability index of each Env variant was calculated by multiplying the CJF-III-288 IC_{50} values (in µM) by the half-life (in days) of virus infectivity at 0°C (on ice). Correlations between the pretriggered Env stability index and other HIV-1 properties are shown.

(F) Correlation between the SIM.2 IC_{50} and the relative infectivity of viruses pseudotyped with the indicated Envs is shown.

Spearman rank-order coefficient (r_S) and two-tailed probability (P) are reported. The names of the HIV-1_{AD8} Env mutants are abbreviated as follows: TF, Tri FPPR; AE, K59A/N136E; AA, K59A/T138A; AR, K59A/K574R; ER, N136E/K574R; WR, A316W/K574R; AER, K59A/N136E/K574R; AWR, K59A/A316W/K574R. See also Tables S3 and S4.

differences in bNAb or pNAb binding to these two Envs were detected. The mature (cleaved) Tri Bam and Tri FPPR Bam Envs were recognized efficiently by bNAbs but much less efficiently by pNAbs. Apparently, the mature Tri Bam Env already exhibits a sufficiently high level of conformational stability so that the addition of the FPPR changes did not result in detectable improvement in the antigenic profile.

Next, we compared the antigenicity of the Tri FPPR Bam Env with those of Tri FPPR Bam Envs with double and triple combinations of K59A, N136E, and K574R changes. These combination mutants exhibited high levels of Env processing, mature Env in virions, and resistance to CD4mcs and cold (see the aforementioned text). In these antigenicity assays, we focused on pNAbs, the binding of which correlates strongly with Env triggerability.[90] Immunoprecipitated Envs were deglycosylated with PNGase F to allow clear separation and easier quantification of

the gp160 and gp120 bands. Compared with the parental Tri FPPR Bam Env, Tri FPPR Bam Envs containing the K574R change exhibited reduced pNAb-gp120 binding (Figure S4B). We confirmed that these mature Tri FPPR Bam Envs with additional modifications were still recognized efficiently by bNAbs (Figure S4C). Thus, the Tri FPPR Bam Env derivatives exhibit an antigenic profile consistent with a stable pretriggered conformation.

Antibody neutralization of stabilized HIV-1_{AD8} Env variants

We compared the sensitivity of pseudoviruses with the wt and stabilized mutant Envs to neutralization by sCD4-Ig and a panel of bNAbs and pNAbs (Figure 5). Compared with the wt AD8 virus, the Tri FPPR, Tri FPPR-K59A/K574R, and Tri FPPR-N136E/K574R viruses were resistant to sCD4-Ig and were slightly more sensitive to most bNAbs (Figure 5A). One exception was the b12 CD4-binding site (CD4BS) bNAb, which neutralized the wt HIV-1_{AD8} slightly more efficiently than the viruses with stabilized Envs. Among the CD4BS bNAbs, b12 exhibits a preference to bind a default intermediate conformation that is more open than the pretriggered conformation.[62,89,117–119] All four viruses were resistant to neutralization by pNAbs directed against the gp120 CD4BS, CD4i, and V2 epitopes (Table S4), with the following exception. The Tri FPPR-N136E/K574R virus and, to a lesser extent, the Tri FPPR-K59A/K574R virus were partially neutralized by high concentrations of pNAbs (447-52D, 39F, and 19b) directed against the gp120 V3 region (Figure 5B). This was unexpected, as the wt AD8 virus is resistant to neutralization by these V3 pNAbs and pretriggered Env stabilization has been shown to decrease the spontaneous exposure of these and other pNAb epitopes.[90] Moreover, our analysis of the antigenicity of the mature Tri FPPR-N136E/K574R and Tri FPPR-K59A/K574R Envs on virus particles did not detect exposure of V3 pNAb epitopes (Figure S4B). These observations argue against the spontaneous exposure of the gp120 V3 loop as a consequence of the additional changes in the Tri FPPR-N136E/K574R and Tri FPPR-K59A/K574R Env mutants.

We considered an alternative explanation for the increased sensitivity of the Tri FPPR-N136E/K574R and Tri FPPR-K59A/K574R viruses to neutralization by V3 antibodies. If changes that stabilize the pretriggered state also increase the stability of functional Env intermediates induced by the engagement of CD4 on the target cell, such intermediates might be accessible to antibodies against V3, which is exposed upon CD4 binding.[120–123] To test this hypothesis, we conducted virus neutralization assays to assess whether the V3 antibodies neutralized the stabilized HIV-1_{AD8} variants by binding the viral Env prior to or after virus engagement of the target cell. We included VRC01, a bNAb directed against the gp120 CD4BS, and two MPER-directed bNAbs, 2F5 and 10E8.v4, in these experiments.

In the assay to evaluate the ability of the antibody to bind the viral Env prior to target cell engagement, the virus was incubated with antibody and pelleted. After removal of the supernatant, the virus was added to target cells and infection was measured (Figure 5C). In this assay format, only VRC01 neutralized the viruses with the wt AD8, Tri FPPR, Tri FPPR-K59A/K574R, and Tri FPPR-N136E/K574R Envs. The V3 pNAbs and MPER bNAbs did not inhibit infection of these viruses in this assay. Thus, these antibodies do not efficiently neutralize cell-free virus prior to engagement of the target cell.

In the assay to evaluate the ability of the antibody to neutralize the virus after it attaches to the cell, viruses were incubated with target cells. After washing the cells, antibody was added and infection was measured (Figure 5D). In this assay format, all four viruses were neutralized by the VRC01 and MPER bNAbs, as expected.[124] The 2F5 and 10E8.v4 bNAbs neutralized the viruses with the Tri FPPR-K59A/K574R and Tri FPPR-N136E/K574R Envs more efficiently than the viruses with the wt AD8 and Tri FPPR Envs. The V3 pNAbs neutralized the viruses with the stabilized Envs (particularly the Tri FPPR-N136E/K574R and Tri FPPR-K59A/K574R Envs) but not the virus with the wt AD8 Env. The 447-52D and 39F pNAbs neutralized the viruses with the stabilized Envs more effectively than the 19b pNAb. These results suggest that after engaging the target cell, intermediates of the stabilized pretriggered Envs are both functional and able to be accessed by certain V3-directed antibodies. This is not the case for the wt AD8 Env intermediates, which either do not contribute significantly to infection or are sterically or temporally inaccessible to pNAbs.[43] Consistent with the former hypothesis, the efficiency with which the stabilized Envs mediated infection, relative to that of the wt AD8 Env, was greater in this assay format than in the cell-free virus neutralization assay shown in Figure 5C. In addition, Envs stabilized in a pretriggered state may engage the multiple CD4 molecules required to establish steric blocks to V3 antibody binding[43] less efficiently than the wt HIV-1_{AD8} Env. Indeed, rates of cell-cell fusion and virus entry were inversely related to pretriggered Env stability (Figure S5). In summary, after virus-target cell engagement, functional intermediates formed by the stabilized pretriggered Envs expose certain V3 elements to antibodies.

Phenotypes of other HIV-1 strains with stabilized pretriggered Envs

We examined whether the Env changes that stabilized the pretriggered conformation of the HIV-1_{AD8} Env would result in similar phenotypes in other HIV-1 strains: HIV-$1_{Du422.1}$ (clade C), HIV-1_{191859} (clade D), and HIV-1_{JR-FL} (clade B).[125–127] Where the wt Env of these HIV-1 strains already had a residue associated with pretriggered Env stability (e.g., Met 535 in JR-FL; Gln 543 in Du422.1 and 191859), these were retained. Stabilization of the HIV-1_{AD8} pretriggered Env by the N136E and T138A changes results from the loss of a gp120 V1 glycan[110]; the position of this glycosylation site shifts in the different HIV-1 strains, so the nearest glycan-modified Asn in each case was changed to Glu. The combined changes introduced into the 191859 and Du422.1 Envs moderately reduced their ability to mediate virus entry (Figure 6), whereas infectivity was severely impaired for the JR-FL Env mutants (data not shown). The processing and subunit association of the Env mutants from all three HIV-1 strains were as good or better than those of the respective wt Envs. As the Du422.1 and 191859 mutant viruses were competent for replication, they were tested for sensitivity to the CJF-III-288 CD4mc and cold inactivation. All the Du422.1 and 191859 mutant viruses were significantly resistant to CJF-III-288, cold, and the combination of CJF-III-288+cold. In the more stringent CJF-III-288+cold assay, the infectivities of the Du422.1 and 191859 mutants with multiple stabilizing Env changes exhibited the longest half-lives. The Du422.1 and 191859 mutant viruses inefficiently infected CD4-negative, CCR5-expressing cells in the presence of CJF-III-288 (Figures S3B and S3C). No

A

Env ligand / Env	IC_{50} (μg/mL)										
	CD4	CD4BS			V2q		gp120-gp41 interface		V3 glycan	gp41 MPER	
	sCD4-Ig	VRC01	VRC03	b12	PG16	PGT145	PGT151	35O22	PGT121	2F5	10E8.v4
wt AD8	1.47 ± 0.39	1.13 ± 0.65	0.15 ± 0.05	0.44 ± 0.18	0.11 ± 0.02	0.20 ± 0.01	0.10 ± 0.02	0.30 ± 0.23	0.13 ± 0.00	> 10	> 9
Tri FPPR	> 50	0.21 ± 0.07	0.03 ± 0.02	0.55 ± 0.12	0.03 ± 0.00	0.07 ± 0.01	0.02 ± 0.01	0.03 ± 0.02	0.09 ± 0.01	6.82 ± 3.50	3.24 ± 0.62
Tri FPPR-K59A/K574R	> 50	0.36 ± 0.04	0.09 ± 0.01	1.98 ± 0.67	0.03 ± 0.02	0.07 ± 0.01	0.02 ± 0.00	0.01 ± 0.01	0.08 ± 0.04	1.89 ± 0.49	0.59 ± 0.14
Tri FPPR-N136E/K574R	> 50	0.30 ± 0.04	0.06 ± 0.01	1.19 ± 0.11	0.06 ± 0.05	0.06 ± 0.02	0.03 ± 0.01	0.02 ± 0.01	0.02 ± 0.01	1.73 ± 0.32	0.66 ± 0.15

Increase Decrease

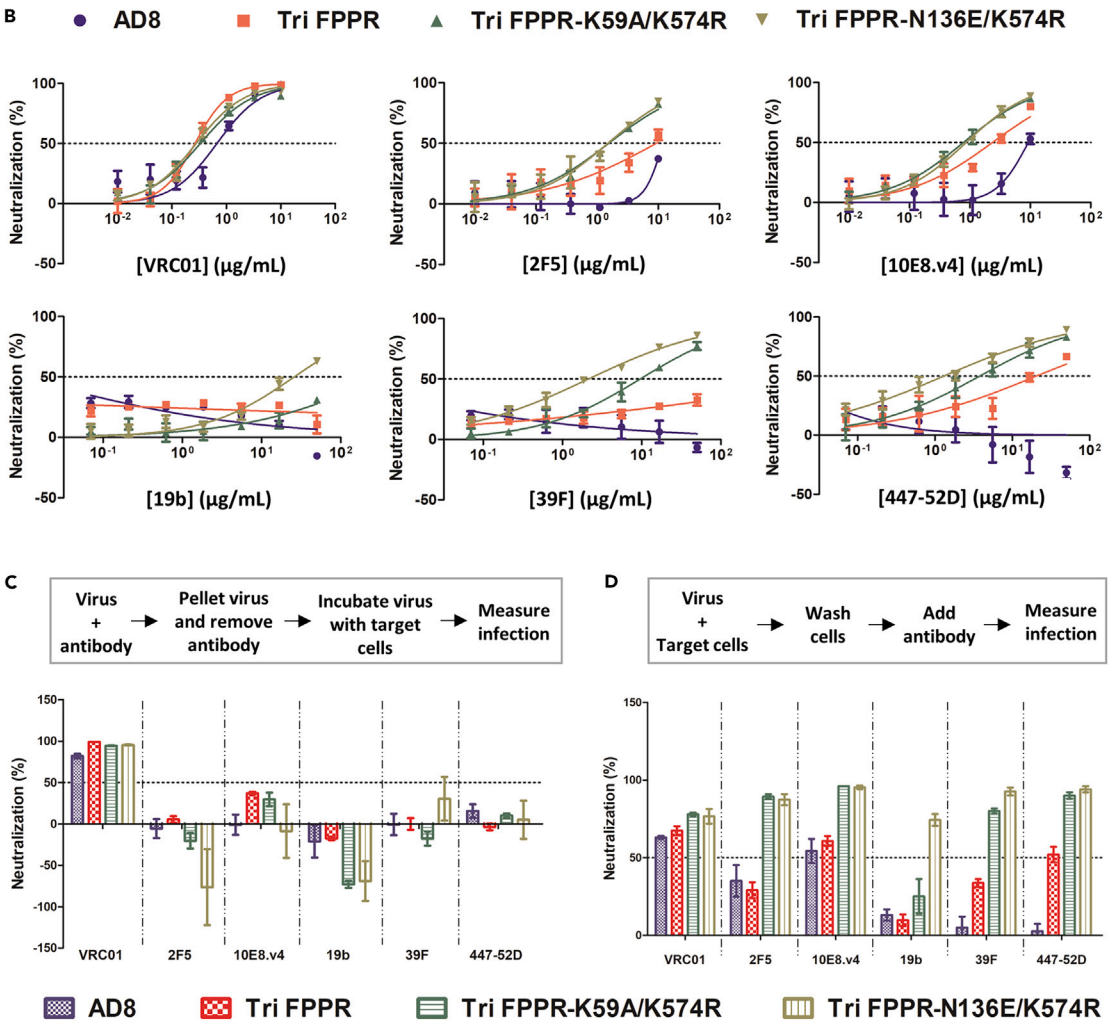

Figure 5. Sensitivity of viruses with stabilized Envs to neutralization by sCD4-Ig and antibodies

(A) Recombinant luciferase-expressing viruses pseudotyped with the indicated Env variants were evaluated for sensitivity to sCD4-Ig and bNAb neutralization. The 50% inhibitory concentration (IC_{50}) values of the Env ligands are reported in μg/mL. Relative to viruses with wt HIV-1_{AD8} Env, increases (green) or decreases (red) in virus sensitivity to inhibition are indicated.

(B) Assays measuring neutralization of the viruses pseudotyped with wt AD8 Env or Tri FPPR variant Envs by a CD4BS bNAb (VRC01), MPER bNAbs (2F5 and 10E8.v4), and V3 pNAbs (19b, 39F, and 447-52D) are shown.

(C) In an assay to measure the ability of antibodies to neutralize cell-free viruses, recombinant viruses pseudotyped with the indicated Envs were incubated for 1 h at 37°C with the following concentrations of antibodies: VRC01 (10 μg/mL), 2F5 and 10E8.v4 (20 μg/mL), 19b, 39F, and 447-52D (50 μg/mL). The viruses were then pelleted and the antibody-containing supernatants were removed. The virus pellet was resuspended in antibody-free medium and incubated with TZM-bl cells in the presence of 20 μg/mL DEAE-dextran. 48 h later, luciferase activity was measured.

(D) In an assay to measure the ability of antibodies to neutralize virus after virus-cell interaction, recombinant viruses pseudotyped with the indicated Envs were added to TZM-bl cells. The virus-cell mixtures were centrifuged at 1800 × g for 30 min at room temperature. The medium was removed and replaced with fresh medium containing the antibody. The antibody concentrations were the same as in (C) above. 48 h later, luciferase activity in the TZM-bl cells was measured. For (A–D), the means and standard deviations derived from at least two independent experiments are shown. See also Figures S4 and S5 and Table S4.

significant differences between the sensitivities of the wt and mutant viruses to the SIM.2 anti-CD4 antibody or maraviroc were observed (Tables S3 and S4). The Du422.1 and 191859 mutant viruses were more resistant to neutralization by sCD4-Ig than the respective wt viruses (Table S5). The wt Du422.1 virus was not neutralized by up to 10 μg/mL of the VRC01, PGT145, and 2F5 bNAbs. By comparison, the Du422.1 viruses with the introduced Env changes were more sensitive to neutralization by the PGT145, PGT151, PGT121, and 10E8.v4 bNAbs. The wt 191859 virus was resistant to the bNAbs tested, except for PGT145. The 191859 Tri FPPR-K59A/K574R virus was neutralized by several bNAbs, including VRC01, PGT151, 2F5, and 10E8.v4. Thus, the phenotypes of the HIV-$1_{Du422.1}$ and HIV-1_{191859} viruses with the introduced Env modifications recapitulated many of the properties observed for the stabilized pretriggered HIV-1_{AD8} mutants.

As the viruses pseudotyped with the HIV_{JR-FL} Envs containing multiple changes replicated poorly, we studied the gp120 shedding propensity and antigenicity of the Env trimers on virus particles. Virions were produced by transfecting HEK293T cells with the pNL4-3.JR-FL E168K plasmid encoding the JR-FL E168K Env and mutant derivatives; the E168K change allows V2 quaternary bNAbs (PG16 and PGT145) against the Env trimer apex to recognize the HIV-1_{JR-FL} Env.[128] The Tri and Tri L543Q changes increased the percentage of cleaved JR-FL E168K Env on virus particles, whereas a slight decrease in the processing of the JR-FL E168K Tri FPPR Env was apparent (Figures S6A and S6C). JR-FL Env mutants with the Tri changes exhibited significantly reduced gp120 shedding in response to BNM-III-170 (Figure S6B and S6C). No significant difference in antigenicity was observed between the JR-FL E168K Env and JR-FL E168K Tri Env, although a small reduction in the precipitation of the JR-FL E168K Tri gp41 by some pNAbs was observed (Figure S6D). When the virion Envs recognized by the antibodies were deglycosylated, the cleaved JR-FL E168K Envs with Tri and Tri L543Q changes exhibited reductions in pNAb binding (Figure S6E). Apparently, the Tri and L543Q changes specify phenotypes in the HIV-1_{JR-FL} Env consistent with those observed in the HIV-1_{AD8} Env.

DISCUSSION

Natural polymorphisms in HIV-1 Env have been identified that can modulate the stability of the pretriggered conformation and thereby regulate the triggerability of the functional Env trimer.[32,33,110,113–115] Many (but not all) of the identified stabilizing Env changes were found to be additive, allowing us to generate membrane Envs stabilized in pretriggered conformations to degrees beyond those found in natural HIV-1 strains. The availability of these unique Env variants provided an opportunity to understand the potential advantages and liabilities to HIV-1 of stabilizing the pretriggered Env conformation with respect to several biological properties, as discussed in the following sections.

Env processing

Previous observations that treatment of Env-expressing cells with BMS-806, which stabilizes a pretriggered Env conformation,[16,22,23,94,104] resulted in decreased Env processing suggested that conformational flexibility of the gp160 Env precursor contributes to cleavage efficiency.[7] Throughout our efforts to stabilize the pretriggered conformation of membrane Envs, we have avoided Env changes that decrease proteolytic processing. The stabilized pretriggered Envs reported here are processed as well or better than their wt counterparts, indicating that stabilization of the functional Env in a pretriggered conformation need not compromise cleavage efficiency. These observations can be reconciled if Env cleavage itself contributes to the stabilizing effects of the introduced Env changes on the pretriggered conformation, a model supported by the differential effects of the Env changes on the antigenicity of cleaved and uncleaved Envs (Figures S4 and S6).[90]

Subunit association and Env spike stability

Resistance of the Env trimer to subunit dissociation and gp120 shedding, either spontaneous or cold-induced, correlated with stabilization of pretriggered Env. Maintenance of a pretriggered conformation may necessitate securing the intersubunit interfaces on the trimer. As discussed in the text further, increased Env spike stability could benefit HIV-1 infection in some circumstances and could also influence Env immunogenicity. For example, resistance of Env to cold inactivation was associated with decreased elicitation of autologous neutralizing antibody responses in monkeys infected with closely matched simian-human immunodeficiency viruses.[129]

Env	Processing	Subunit association	Cell-cell fusion (%)	Infectivity (%)	IC_{50} (μM) CJF-III-288	Cold ($t_{1/2}$) (days)	$t_{1/2}$ (days) (CD4mc + cold)
Du422.1	1	1	100	100.0	6.0 ± 1.13	4.5 ± 1.3	<0.04
Du422.1 Tri	1.61 ± 0.09	0.66 ± 0.29	75 ± 12	31.1 ± 5.24	13.47 ± 4.9	>14	<0.04
Du422.1 Tri-I535M	1.49 ± 0.89	1.13 ± 0.09	ND	36.1 ± 0.48	14.04 ± 2.9	>14	0.4 ± 0.01
Du422.1 Tri FPPR (A532V/I535M/Q543Q)	1.81 ± 0.37	1.06 ± 0.14	43 ± 8	23.9 ± 5.58	24.24 ± 1.05	>14	0.53 ± 0.01
Du422.1 Tri FPPR (A532V/I535M/Q543N)	2.00 ± 0.32	1.34 ± 0.51	ND	16.5 ± 6.06	16.73 ± 1.81	>14	0.65 ± 0.02
Du422.1 Tri FPPR-K59A	2.34 ± 0.64	1.06 ± 0.21	ND	33.5 ± 4.19	77.56 ± 2.2	>14	>14
Du422.1 Tri FPPR-N135E	2.21 ± 0.68	1.14 ± 0.71	ND	30.1 ± 3.89	94.83 ± 1.65	>14	>14
Du422.1 Tri FPPR-K574R	1.91 ± 0.50	2.17 ± 0.48	ND	27.6 ± 2.55	129.55 ± 6.29	>14	>14
Du422.1 Tri FPPR-K59A/N135E	1.79 ± 0.47	1.64 ± 0.81	ND	22.2 ± 2.92	105.19 ± 9.63	>14	>14
Du422.1 Tri FPPR-K59A/K574R	1.75 ± 0.40	1.21 ± 0.46	39 ± 5	27.2 ± 2.65	101.03 ± 4.20	>14	>14
Du422.1 Tri FPPR-N135E/K574R	1.83 ± 0.44	1.80 ± 0.69	ND	17.1 ± 2.86	148.41 ± 46.2	>14	>14
Du422.1 Tri FPPR-K59A/N135E/K574R	2.30 ± 0.89	2.49 ± 0.89	40 ± 8	12.2 ± 6.07	>200	>14	>14
191859	1	1	100	100.0	11.48 ± 2.09	0.25 ± 0.03	<0.04
191859 Tri	1.23 ± 0.51	1.12 ± 0.31	122 ± 6	73.5 ± 9.85	73.02 ± 0.45	>9	<0.04
191859 Tri-L535M	1.18 ± 0.46	0.63 ± 0.15	ND	72.8 ± 5.16	42.62 ± 3.71	>9	<0.04
191859 Tri FPPR-(A532V/L535M/Q543Q)	1.49 ± 0.42	1.09 ± 0.38	106 ± 12	44.4 ± 20.15	50.61 ± 2.82	>9	<0.04
191859 Tri FPPR-(A532V/L535M/Q543N)	2.53 ± 0.83	1.34 ± 0.35	ND	36.3 ± 11.21	54.51 ± 3.54	>9	<0.04
191859 Tri FPPR-K59A	1.79 ± 0.39	1.91 ± 0.39	ND	39.9 ± 8.16	49.98 ± 4.21	>9	<0.04
191859 Tri FPPR-N139E	1.46 ± 0.29	1.58 ± 0.33	ND	28.4 ± 12.94	101.35 ± 0.92	>9	<0.04
191859 Tri FPPR-K574R	2.08 ± 0.53	2.24 ± 0.61	ND	24.9 ± 10.71	100.06 ± 6.99	>9	0.9 ± 0.01
191859 Tri FPPR-K59A/N139E	2.48 ± 78	1.42 ± 0.30	ND	40.5 ± 7.72	71.65 ± 1.92	>9	0.08 ± 0.01
191859 Tri FPPR-K59A/K574R	1.90 ± 0.74	1.49 ± 0.11	120 ± 23	28.9 ± 12.30	105.70 ± 8.92	>9	2.3 ± 0.9
191859 Tri FPPR-N139E/K574R	1.64 ± 0.88	1.56 ± 0.84	ND	36.4 ± 13.61	188.55 ± 10.54	>9	2.1 ± 0.08
191859 Tri FPPR-K59A/N139E/K574R	1.79 ± 0.77	2.06 ± .87	116 ± 8	37.3 ± 0.61	164 ± 16.97	>9	2.1 ± 0.09

IC_{50} (μM)	0-50	50-100	100-200	>200
Days	< 0.04	0.04-1	1-14	> 14

Figure 6. Effects of stabilizing changes on the phenotypes of viruses with Envs from clade C and D HIV-1 strains

Env processing, subunit association, cell-cell fusing ability, and virus infectivity are shown for the wt and variant HIV-$1_{DU422.1}$ (clade C) and HIV-1_{191859} (clade D) Envs, normalized to those values observed for the respective wt Env. The sensitivity of viruses pseudotyped with the Env variants to inhibition by the CJF-III-288 CD4mc, exposure to cold (0°C), or combined exposure to CJF-III-288 + cold is shown, as detailed in the legend of Figure 2. Values are colored according to the key. Note that the wt Du422.1 and 191859 Envs have a glutamine residue at 543, which was retained in the Tri FPPR variants (except for Tri FPPR(N), in which residue 543 is an asparagine). See also Figures S3 and S6 and Tables S4 and S5.

Env function in mediating membrane fusion and virus entry

Decreased triggerability negatively impacted Env-mediated cell-cell fusion and virus entry. In the absence of offsetting advantages with respect to immune evasion, decreased triggerability would presumably be counterselected in primary HIV-1 strains. As the level of CD4 on the target cells can influence the phenotypic effects of altered triggerability on virus entry,[17,30] primary HIV-1 strains are expected to retain sufficient triggerability to infect available target cells. Based on virus sensitivity to cold and CD4mc inhibition, most primary HIV-1 strains have evolved Envs with considerably greater triggerability than that of our more stabilized Env variants. Among the primary HIV-1 examined, the CAP45.200.G3 Env was unusually resistant to cold and CD4mcs, consistent with low triggerability; perhaps, as a consequence, the CAP45.200.G3 pseudoviruses were poorly infectious. We found that the degree to which the stabilizing changes compromised Env function differed among HIV-1 strains, an observation worthy of future investigation.

Susceptibility to antibody neutralization

Consistent with the preferred recognition of the pretriggered Env conformation by most bNAbs, viruses with Envs stabilized in a pretriggered state were often neutralized by bNAbs better than the wt parental viruses. Given the low frequency and titer at which bNAbs are elicited during natural HIV-1 infection, this potential liability may have little practical consequences. We note that relative to the wt HIV-1_{AD8}, viruses with Envs stabilized in a pretriggered state were more resistant to sCD4-Ig and the b12 bNAb, which preferentially recognize more open conformations.[118,119] The b12 bNAb has been suggested to bind an asymmetric Env trimer representative of the default intermediate state.[89] The viruses with HIV-1_{AD8} Envs that were highly stabilized in a pretriggered state exhibited increased sensitivity to MPER bNAbs, relative to the wt HIV-1_{AD8}. This was unexpected, since MPER bNAbs are thought to neutralize by recognizing CD4-bound conformations of Env.[124] We confirmed that neutralization by MPER bNAbs occurs after engagement of the target cell by the wt HIV-1_{AD8} and showed that this was also the case for the highly stabilized Env mutants. As discussed in the following text, these observations imply that changes that stabilize the pretriggered Env also increase the access of certain antibodies to a functional Env intermediate in the virus entry process.

The high titers of pNAbs generated in nearly all HIV-1-infected individuals make their avoidance of great practical importance to the virus.[42–44,48,49] Primary HIV-1 strains and most of the stabilized pretriggered Env mutants studied here resist neutralization by pNAbs. Surprisingly, compared with the wt HIV-1_{AD8}, the HIV-1_{AD8} Env variants highly stabilized in a pretriggered state exhibited increased sensitivity specifically to V3-directed pNAbs. As for the MPER bNAbs discussed earlier, neutralization by the V3 pNAbs occurred after engagement of the target cell by the virus. These observations suggest that the changes that stabilize the pretriggered Env increase the availability of a functional Env intermediate to V3 pNAbs and MPER bNAbs (Figures 7 and S7).

The weak binding of pNAbs to the mature Env trimers of some primary HIV-1 strains (including HIV-1_{AD8} and HIV-1_{JR-FL} herein) results from the spontaneous sampling of more open Env conformations; this conclusion is supported by the observation that such pNAb binding is decreased by Env changes that stabilize the pretriggered conformation or by treatment of Env with crosslinkers or BMS-806.[16,23,32,39,88–90] The observed pNAb binding may be reconciled with the lack of virus neutralization by these pNAbs if such open Env conformers are functionally labile and contribute only minimally to virus infectivity.[90] Likewise, open Envs initially bound by CD4 are only transiently activated and may irreversibly decay if additional receptor engagement is delayed.[28] Stabilization of the pretriggered Env may increase the functional longevity of the initial CD4-bound Env intermediate and may slow the subsequent binding of additional CD4 molecules (Figure 7). The slower kinetics of cell-cell and virus-cell membrane fusion mediated by stabilized pretriggered Envs supports this model (Figure S5). Once the full-CD4-bound conformation is achieved, Env epitopes recognized by V3 and CD4i pNAbs are sterically occluded.[43] On the stabilized Env intermediates, only V3 pNAb epitopes are exposed and not those of other pNAbs, including CD4i pNAbs (Figure S7; Table S4). The exposure of the gp120 V3 region is apparently partial, as not all V3-directed pNAbs show the same degree of neutralization and high concentrations of the pNAbs are required to achieve even 50% neutralization. Nonetheless, the results reveal another potential liability that could lead to natural counterselection of HIV-1 variants with highly stabilized pretriggered Envs.

Our results provide valuable insights into the advantages and disadvantages of HIV-1 modulating the stability of the pretriggered Env conformation. Env mutants stabilized in a pretriggered state should expedite determination of the structure and immunogenicity of this functionally important Env conformation.

Limitations of the study

In this study, the stability of the pretriggered HIV-1 Env conformation was evaluated using functional, antigenic, and structural correlates. It would be valuable to relate the stabilized Env conformations to those states defined by single-molecule fluorescence resonance energy transfer and to assess the effects of the introduced Env changes on the rates of transitions between conformations. The wide range of effects of the stabilizing Env changes on the infectivity of different HIV-1 strains merits further study. Evaluation of the structure and immunogenicity of the stabilized Envs will require additional studies.

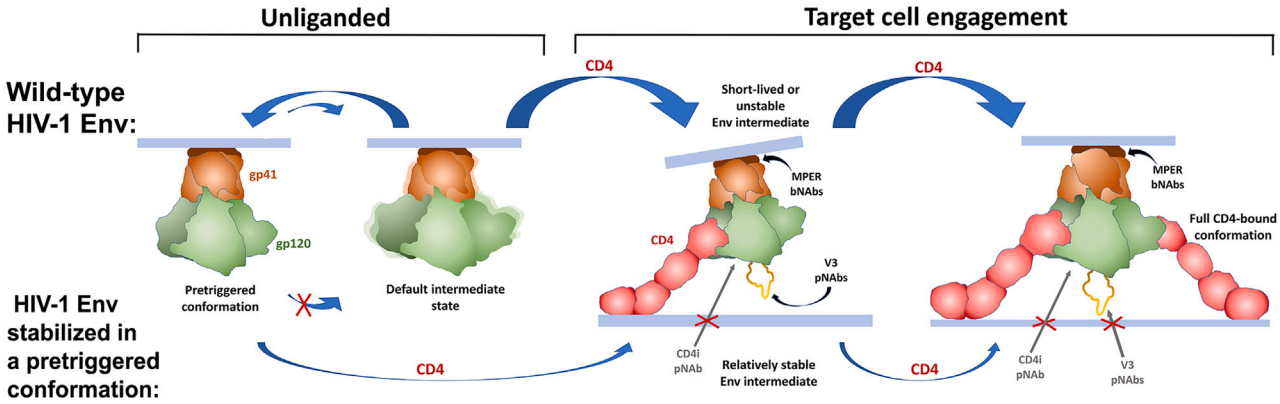

Figure 7. Effects of pretriggered Env stabilization on HIV-1 infectivity and susceptibility to antibody neutralization

A wt HIV-1 Env and an Env that is highly stabilized in a pretriggered conformation are compared in unliganded states or following engagement of the virus with a $CD4^+$ target cell. In the absence of ligands, the Envs of primary HIV-1 largely occupy the pretriggered conformation but, depending on their triggerability, also sample more open conformations, some of which are recognized by pNAbs (default intermediate state). Env changes that stabilize the pretriggered conformation limit the spontaneous sampling of conformations recognized by pNAbs and decrease Env triggerability by CD4. Upon the initial engagement with a single CD4 molecule on the target cell, Env exposes V3, CD4i, and MPER epitopes. wt HIV-1 Envs either engage additional CD4 molecules or undergo inactivation. Once multiple CD4 molecules are bound, the V3 and CD4i epitopes are sterically occluded by the target membrane, whereas the MPER epitopes remain available for the binding of bNAbs.[43,124] For Envs stabilized in a pretriggered conformation, transitions after the initial binding of a single CD4 molecule are less efficient, slowing establishment of the sterically protected full CD4-bound conformation and decreasing functional inactivation by events such as gp120 shedding. The prolonged presence of a more stable functional Env intermediate with less-than-complete occupancy by CD4 increases the opportunity for neutralization by V3-directed pNAbs. The efficacy of MPER bNAbs, which also recognize this Env intermediate, is likewise enhanced. Note that the binding of CD4i pNAbs is likely to be sterically blocked even in the case of Env bound to a single CD4 molecule. See also Figures S5 and S7.

STAR★METHODS

Detailed methods are provided in the online version of this paper and include the following:

- KEY RESOURCES TABLE
- RESOURCE AVAILABILITY
  - Lead contact
  - Materials availability
  - Data and code availability
- METHOD DETAILS
  - HIV-1 Env mutants
  - Antibodies, sCD4-Ig and small-molecule HIV-1 entry inhibitors
  - Cell lines
  - Env expression
  - Cell-cell fusion assay
  - Virus infectivity
  - Kinetics of cell-cell fusion and virus entry
  - Activation of virus infection by CD4mcs
  - Virus sensitivity to cold inactivation
  - Virus inhibition/neutralization
  - Virus sensitivity to combined exposure to a CD4mc and 0°C
  - Analysis of Env on infectious virus particles produced from proviral clones
  - Shedding of gp120 from virus particles
  - Antigenicity of Env on virus particles
- QUANTIFICATION AND STATISTICAL ANALYSIS

SUPPLEMENTAL INFORMATION

Supplemental information can be found online at https://doi.org/10.1016/j.isci.2024.110141.

ACKNOWLEDGMENTS

We thank Ms. Elizabeth Carpelan for manuscript preparation. This work was supported by grants from the National Institutes of Health (grant nos. AI145547, AI124982, AI150471, AI129017, AI164562, AI176904, and AI178833), a grant from Gilead Sciences, by Michael Siff Funds for Basic Research (Dana-Farber Cancer Institute), and by a gift from the late William F. McCarty-Cooper.

AUTHOR CONTRIBUTIONS

Conceptualization, Z.Z., S.A., H.T.N., and J.G.S.; investigation, Z.Z., S.A., and H.T.N.; resources, C.F. and A.B.S. III; writing – original draft, H.T.N., S.A., Z.Z., and J.G.S.; writing – review and editing, Z.Z., S.A., H.T.N., C.F., A.B.S. III, and J.G.S.; supervision, A.B.S. III, H.T.N., and J.G.S.; funding acquisition, A.B.S. III and J.G.S.

DECLARATION OF INTERESTS

A patent application covering stabilized pretriggered membrane HIV-1 envelope glycoproteins has been submitted.

Received: January 10, 2024
Revised: April 8, 2024
Accepted: May 27, 2024
Published: May 28, 2024

REFERENCES

1. Wyatt, R., and Sodroski, J. (1998). The HIV-1 envelope glycoproteins: fusogens, antigens, and immunogens. Science *280*, 1884–1888. https://doi.org/10.1126/science.280.5371.1884.
2. Chen, B. (2019). Molecular mechanism of HIV-1 entry. Trends Microbiol. *27*, 878–891. https://doi.org/10.1016/j.tim.2019.06.002.
3. Willey, R.L., Bonifacino, J.S., Potts, B.J., Martin, M.A., and Klausner, R.D. (1988). Biosynthesis, cleavage, and degradation of the human immunodeficiency virus 1 envelope glycoprotein gp160. Proc. Natl. Acad. Sci. USA *85*, 9580–9584. https://doi.org/10.1073/pnas.85.24.9580.
4. Earl, P.L., Moss, B., and Doms, R.W. (1991). Folding, interaction with GRP78-BiP, assembly, and transport of the human immunodeficiency virus type 1 envelope protein. J. Virol. *65*, 2047–2055. https://doi.org/10.1128/JVI.65.4.2047-2055.1991.
5. Pal, R., Hoke, G.M., and Sarngadharan, M.G. (1989). Role of oligosaccharides in the processing and maturation of envelope glycoproteins of human immunodeficiency virus type 1. Proc. Natl. Acad. Sci. USA *86*, 3384–3388. https://doi.org/10.1073/pnas.86.9.3384.
6. Dewar, R.L., Vasudevachari, M.B., Natarajan, V., and Salzman, N.P. (1989). Biosynthesis and processing of human immunodeficiency virus type 1 envelope glycoproteins: effects of monensin on glycosylation and transport. J. Virol. *63*, 2452–2456. https://doi.org/10.1128/JVI.63.6.2452-2456.1989.
7. Zhang, S., Nguyen, H.T., Ding, H., Wang, J., Zou, S., Liu, L., Guha, D., Gabuzda, D., Ho, D.D., Kappes, J.C., and Sodroski, J. (2021). Dual pathways of human immunodeficiency virus type 1 envelope glycoprotein trafficking modulate the selective exclusion of uncleaved oligomers from virions. J. Virol. *95*, e01369-20. https://doi.org/10.1128/JVI.01369-20.
8. Stein, B.S., and Engleman, E.G. (1990). Intracellular processing of the gp160 HIV-1 envelope precursor. Endoproteolytic cleavage occurs in a cis or medial compartment of the Golgi complex. J. Biol. Chem. *265*, 2640–2649.
9. Merkle, R.K., Helland, D.E., Welles, J.L., Shilatifard, A., Haseltine, W.A., and Cummings, R.D. (1991). gp160 of HIV-I synthesized by persistently infected Molt-3 cells is terminally glycosylated: evidence that cleavage of gp160 occurs subsequent to oligosaccharide processing. Arch. Biochem. Biophys. *290*, 248–257. https://doi.org/10.1016/0003-9861(91)90616-q.
10. Klatzmann, D., Champagne, E., Chamaret, S., Gruest, J., Guetard, D., Hercend, T., Gluckman, J.C., and Montagnier, L. (1984). T-lymphocyte T4 molecule behaves as the receptor for human retrovirus LAV. Nature *312*, 767–768. https://doi.org/10.1038/312767a0.
11. Dalgleish, A.G., Beverley, P.C., Clapham, P.R., Crawford, D.H., Greaves, M.F., and Weiss, R.A. (1984). The CD4 (T4) antigen is an essential component of the receptor for the AIDS retrovirus. Nature *312*, 763–767. https://doi.org/10.1038/312763a0.
12. Wu, L., Gerard, N.P., Wyatt, R., Choe, H., Parolin, C., Ruffing, N., Borsetti, A., Cardoso, A.A., Desjardin, E., Newman, W., et al. (1996). CD4-induced interaction of primary HIV-1 gp120 glycoproteins with the chemokine receptor CCR-5. Nature *384*, 179–183. https://doi.org/10.1038/384179a0.
13. Trkola, A., Dragic, T., Arthos, J., Binley, J.M., Olson, W.C., Allaway, G.P., Cheng-Mayer, C., Robinson, J., Maddon, P.J., and Moore, J.P. (1996). CD4-dependent, antibody-sensitive interactions between HIV-1 and its co-receptor CCR-5. Nature *384*, 184–187. https://doi.org/10.1038/384184a0.
14. Feng, Y., Broder, C.C., Kennedy, P.E., and Berger, E.A. (1996). HIV-1 entry cofactor: functional cDNA cloning of a seven-transmembrane, G protein-coupled receptor. Science *272*, 872–877. https://doi.org/10.1126/science.272.5263.872.
15. Alkhatib, G., Combadiere, C., Broder, C.C., Feng, Y., Kennedy, P.E., Murphy, P.M., and Berger, E.A. (1996). CC CKR5: a RANTES, MIP-1alpha, MIP-1beta receptor as a fusion cofactor for macrophage-tropic HIV-1. Science *272*, 1955–1958. https://doi.org/10.1126/science.272.5270.1955.
16. Munro, J.B., Gorman, J., Ma, X., Zhou, Z., Arthos, J., Burton, D.R., Koff, W.C., Courter, J.R., Smith, A.B., III, Kwong, P.D., et al. (2014). Conformational dynamics of single HIV-1 envelope trimers on the surface of native virions. Science *346*, 759–763. https://doi.org/10.1126/science.1254426.
17. Herschhorn, A., Ma, X., Gu, C., Ventura, J.D., Castillo-Menendez, L., Melillo, B., Terry, D.S., Smith, A.B., III, Blanchard, S.C., Munro, J.B., et al. (2016). Release of gp120 restraints leads to an entry-competent intermediate state of the HIV-1 envelope glycoproteins. mBio *7*, e01598-16. https://doi.org/10.1128/mBio.01598-16.
18. Ma, X., Lu, M., Gorman, J., Terry, D.S., Hong, X., Zhou, Z., Zhao, H., Altman, R.B., Arthos, J., Blanchard, S.C., et al. (2018). HIV-1 Env trimer opens through an asymmetric intermediate in which individual protomers adopt distinct conformations. Elife *7*, e34271. https://doi.org/10.7554/eLife.34271.
19. Chan, D.C., Fass, D., Berger, J.M., and Kim, P.S. (1997). Core structure of gp41 from the HIV envelope glycoprotein. Cell *89*, 263–273. https://doi.org/10.1016/s0092-8674(00)80205-6.
20. Weissenhorn, W., Dessen, A., Harrison, S.C., Skehel, J.J., and Wiley, D.C. (1997). Atomic structure of the ectodomain from HIV-1 gp41. Nature *387*, 426–430. https://doi.org/10.1038/387426a0.
21. Melikyan, G.B., Markosyan, R.M., Hemmati, H., Delmedico, M.K., Lambert, D.M., and Cohen, F.S. (2000). Evidence that the transition of HIV-1 gp41 into a six-helix bundle, not the bundle configuration, induces membrane fusion. J. Cell Biol. *151*, 413–423. https://doi.org/10.1083/jcb.151.2.413.
22. Si, Z., Madani, N., Cox, J.M., Chruma, J.J., Klein, J.C., Schön, A., Phan, N., Wang, L., Biorn, A.C., Cocklin, S., et al. (2004). Small-molecule inhibitors of HIV-1 entry block receptor-induced conformational changes in the viral envelope glycoproteins. Proc.

Natl. Acad. Sci. USA *101*, 5036–5041. https://doi.org/10.1073/pnas.0307953101.
23. Zou, S., Zhang, S., Gaffney, A., Ding, H., Lu, M., Grover, J.R., Farrell, M., Nguyen, H.T., Zhao, C., Anang, S., et al. (2020). Long-acting BMS-378806 analogues stabilize the State-1 conformation of the human immunodeficiency virus type 1 envelope glycoproteins. J. Virol. *94*, e001488-20. https://doi.org/10.1128/JVI.00148-20.
24. Zhao, Q., Ma, L., Jiang, S., Lu, H., Liu, S., He, Y., Strick, N., Neamati, N., and Debnath, A.K. (2005). Identification of N-phenyl-N′-(2,2,6,6-tetramethyl-piperidin-4-yl)-oxalamides as a new class of HIV-1 entry inhibitors that prevent gp120 binding to CD4. Virology *339*, 213–225. https://doi.org/10.1016/j.virol.2005.06.008.
25. Schön, A., Madani, N., Klein, J.C., Hubicki, A., Ng, D., Yang, X., Smith, A.B., III, Sodroski, J., and Freire, E. (2006). Thermodynamics of binding of a low-molecular-weight CD4 mimetic to HIV-1 gp120. Biochemistry *45*, 10973–10980. https://doi.org/10.1021/bi061193r.
26. Melillo, B., Liang, S., Park, J., Schön, A., Courter, J.R., LaLonde, J.M., Wendler, D.J., Princiotto, A.M., Seaman, M.S., Freire, E., et al. (2016). Small-molecule CD4-mimics: Structure-based optimization of HIV-1 entry inhibition. ACS Med. Chem. Lett. *7*, 330–334. https://doi.org/10.1021/acsmedchemlett.5b00471.
27. Fritschi, C.J., Anang, S., Gong, Z., Mohammadi, M., Richard, J., Bourassa, C., Severino, K.T., Richter, H., Yang, D., Chen, H.C., et al. (2023). Indoline CD4-mimetic compounds mediate potent and broad HIV-1 inhibition and sensitization to antibody-dependent cellular cytotoxicity. Proc. Natl. Acad. Sci. USA *120*, e2222073120. https://doi.org/10.1073/pnas.2222073120.
28. Haim, H., Si, Z., Madani, N., Wang, L., Courter, J.R., Princiotto, A., Kassa, A., DeGrace, M., McGee-Estrada, K., Mefford, M., et al. (2009). Soluble CD4 and CD4-mimetic compounds inhibit HIV-1 infection by induction of a short-lived activated state. PLoS Pathog. *5*, e1000360. https://doi.org/10.1371/journal.ppat.1000360.
29. Madani, N., Princiotto, A.M., Zhao, C., Jahanbakhshsefidi, F., Mertens, M., Herschhorn, A., Melillo, B., Smith, A.B., III, and Sodroski, J. (2017). Activation and inactivation of primary human immunodeficiency virus envelope glycoprotein trimers by CD4-mimetic compounds. J. Virol. *91*, e01880-16. https://doi.org/10.1128/JVI.01880-16.
30. Herschhorn, A., Gu, C., Moraca, F., Ma, X., Farrell, M., Smith, A.B., III, Pancera, M., Kwong, P.D., Schön, A., Freire, E., et al. (2017). The β20-β21 of gp120 is a regulatory switch for HIV-1 Env conformational transitions. Nat. Commun. *8*, 1049. https://doi.org/10.1038/s41467-017-01119-w.
31. Haim, H., Strack, B., Kassa, A., Madani, N., Wang, L., Courter, J.R., Princiotto, A., McGee, K., Pacheco, B., Seaman, M.S., et al. (2011). Contribution of intrinsic reactivity of the HIV-1 envelope glycoproteins to CD4-independent infection and global inhibitor sensitivity. PLoS Pathog. *7*, e1002101. https://doi.org/10.1371/journal.ppat.1002101.
32. Nguyen, H.T., Qualizza, A., Anang, S., Zhao, M., Zou, S., Zhou, R., Wang, Q., Zhang, S., Deshpande, A., Ding, H., et al. (2022). Functional and highly cross-linkable HIV-1 envelope glycoproteins enriched in a pretriggered conformation. J. Virol. *96*, e0166821. https://doi.org/10.1128/jvi.01668-21.
33. Pacheco, B., Alsahafi, N., Debbeche, O., Prévost, J., Ding, S., Chapleau, J.P., Herschhorn, A., Madani, N., Princiotto, A., Melillo, B., et al. (2017). Residues in the gp41 ectodomain regulate HIV-1 envelope glycoprotein conformational transitions induced by gp120-directed inhibitors. J. Virol. *91*, e02219-16. https://doi.org/10.1128/JVI.02219-16.
34. Stewart-Jones, G.B.E., Soto, C., Lemmin, T., Chuang, G.Y., Druz, A., Kong, R., Thomas, P.V., Wagh, K., Zhou, T., Behrens, A.J., et al. (2016). Trimeric HIV-1-Env structures define glycan shields from Clades A, B, and G. Cell *165*, 813–826. https://doi.org/10.1016/j.cell.2016.04.010.
35. Bonsignori, M., Liao, H.X., Gao, F., Williams, W.B., Alam, S.M., Montefiori, D.C., and Haynes, B.F. (2017). Antibody-virus co-evolution in HIV infection: paths for HIV vaccine development. Immunol. Rev. *275*, 145–160. https://doi.org/10.1111/imr.12509.
36. Wei, X., Decker, J.M., Wang, S., Hui, H., Kappes, J.C., Wu, X., Salazar-Gonzalez, J.F., Salazar, M.G., Kilby, J.M., Saag, M.S., et al. (2003). Antibody neutralization and escape by HIV-1. Nature *422*, 307–312. https://doi.org/10.1038/nature01470.
37. Ward, A.B., and Wilson, I.A. (2017). The HIV-1 envelope glycoprotein structure: nailing down a moving target. Immunol. Rev. *275*, 21–32. https://doi.org/10.1111/imr.12507.
38. Moore, P.L., Ranchobe, N., Lambson, B.E., Gray, E.S., Cave, E., Abrahams, M.R., Bandawe, G., Mlisana, K., Abdool Karim, S.S., Williamson, C., et al. (2009). Limited neutralizing antibody specificities drive neutralization escape in early HIV-1 subtype C infection. PLoS Pathog. *5*, e1000598. https://doi.org/10.1371/journal.ppat.1000598.
39. Zhang, S., Wang, K., Wang, W.L., Nguyen, H.T., Chen, S., Lu, M., Go, E.P., Ding, H., Steinbock, R.T., Desaire, H., et al. (2021). Asymmetric structures and conformational plasticity of the uncleaved full-length human immunodeficiency virus envelope glycoprotein trimer. J. Virol. *95*, e0052921. https://doi.org/10.1128/JVI.00529-21.
40. Haim, H., Salas, I., and Sodroski, J. (2013). Proteolytic processing of the human immunodeficiency virus envelope glycoprotein precursor decreases conformational flexibility. J. Virol. *87*, 1884–1889. https://doi.org/10.1128/JVI.02765-12.
41. Pancera, M., and Wyatt, R. (2005). Selective recognition of oligomeric HIV-1 primary isolate envelope glycoproteins by potently neutralizing ligands requires efficient precursor cleavage. Virology *332*, 145–156. https://doi.org/10.1016/j.virol.2004.10.042.
42. Haim, H., Salas, I., McGee, K., Eichelberger, N., Winter, E., Pacheco, B., and Sodroski, J. (2013). Modeling virus- and antibody-specific factors to predict human immunodeficiency virus neutralization efficiency. Cell Host Microbe *14*, 547–558. https://doi.org/10.1016/j.chom.2013.10.006.
43. Labrijn, A.F., Poignard, P., Raja, A., Zwick, M.B., Delgado, K., Franti, M., Binley, J., Vivona, V., Grundner, C., Huang, C.C., et al. (2003). Access of antibody molecules to the conserved coreceptor binding site on glycoprotein gp120 is sterically restricted on primary human immunodeficiency virus type 1. J. Virol. *77*, 10557–10565. https://doi.org/10.1128/jvi.77.19.10557-10565.2003.
44. Guttman, M., Cupo, A., Julien, J.P., Sanders, R.W., Wilson, I.A., Moore, J.P., and Lee, K.K. (2015). Antibody potency relates to the ability to recognize the closed, pre-fusion form of HIV Env. Nat. Commun. *6*, 6144. https://doi.org/10.1038/ncomms7144.
45. Gray, E.S., Taylor, N., Wycuff, D., Moore, P.L., Tomaras, G.D., Wibmer, C.K., Puren, A., DeCamp, A., Gilbert, P.B., Wood, B., et al. (2009). Antibody specificities associated with neutralization breadth in plasma from human immunodeficiency virus type 1 subtype C-infected blood donors. J. Virol. *83*, 8925–8937. https://doi.org/10.1128/JVI.00758-09.
46. Sather, D.N., Armann, J., Ching, L.K., Mavrantoni, A., Sellhorn, G., Caldwell, Z., Yu, X., Wood, B., Self, S., Kalams, S., and Stamatatos, L. (2009). Factors associated with the development of cross-reactive neutralizing antibodies during human immunodeficiency virus type 1 infection. J. Virol. *83*, 757–769. https://doi.org/10.1128/JVI.02036-08.
47. Hraber, P., Seaman, M.S., Bailer, R.T., Mascola, J.R., Montefiori, D.C., and Korber, B.T. (2014). Prevalence of broadly neutralizing antibody responses during chronic HIV-1 infection. AIDS *28*, 163–169. https://doi.org/10.1097/QAD.0000000000000106.
48. Walker, L.M., Simek, M.D., Priddy, F., Gach, J.S., Wagner, D., Zwick, M.B., Phogat, S.K., Poignard, P., and Burton, D.R. (2010). A limited number of antibody specificities mediate broad and potent serum neutralization in selected HIV-1 infected individuals. PLoS Pathog. *6*, e1001028. https://doi.org/10.1371/journal.ppat.1001028.
49. Gray, E.S., Madiga, M.C., Hermanus, T., Moore, P.L., Wibmer, C.K., Tumba, N.L., Werner, L., Mlisana, K., Sibeko, S., Williamson, C., et al. (2011). The neutralization breadth of HIV-1 develops incrementally over four years and is associated with CD4+ T cell decline and high viral load during acute infection. J. Virol. *85*, 4828–4840. https://doi.org/10.1128/JVI.00198-11.
50. Hessell, A.J., Poignard, P., Hunter, M., Hangartner, L., Tehrani, D.M., Bleeker, W.K., Parren, P.W.H.I., Marx, P.A., and Burton, D.R. (2009). Effective, low-titer antibody protection against low-dose repeated mucosal SHIV challenge in macaques. Nat. Med. *15*, 951–954. https://doi.org/10.1038/nm.1974.
51. Mascola, J.R., Lewis, M.G., Stiegler, G., Harris, D., VanCott, T.C., Hayes, D., Louder, M.K., Brown, C.R., Sapan, C.V., Frankel, S.S., et al. (1999). Protection of macaques against pathogenic simian/human immunodeficiency virus 89.6PD by passive transfer of neutralizing antibodies. J. Virol. *73*, 4009–4018. https://doi.org/10.1128/JVI.73.5.4009-4018.1999.
52. Mascola, J.R., Stiegler, G., VanCott, T.C., Katinger, H., Carpenter, C.B., Hanson, C.E., Beary, H., Hayes, D., Frankel, S.S., Birx, D.L., and Lewis, M.G. (2000). Protection of macaques against vaginal transmission of a pathogenic HIV-1/SIV chimeric virus by

passive infusion of neutralizing antibodies. Nat. Med. *6*, 207–210. https://doi.org/10.1038/72318.

53. Parren, P.W., Marx, P.A., Hessell, A.J., Luckay, A., Harouse, J., Cheng-Mayer, C., Moore, J.P., and Burton, D.R. (2001). Antibody protects macaques against vaginal challenge with a pathogenic R5 simian/human immunodeficiency virus at serum levels giving complete neutralization in vitro. J. Virol. *75*, 8340–8347. https://doi.org/10.1128/jvi.75.17.8340-8347.2001.
54. Pauthner, M., Havenar-Daughton, C., Sok, D., Nkolola, J.P., Bastidas, R., Boopathy, A.V., Carnathan, D.G., Chandrashekar, A., Cirelli, K.M., Cottrell, C.A., et al. (2017). Elicitation of robust Tier 2 neutralizing antibody responses in nonhuman primates by HIV envelope trimer immunization using optimized approaches. Immunity *46*, 1073–1088.e6. https://doi.org/10.1016/j.immuni.2017.05.007.
55. Torrents de la Peña, A., de Taeye, S.W., Sliepen, K., LaBranche, C.C., Burger, J.A., Schermer, E.E., Montefiori, D.C., Moore, J.P., Klasse, P.J., and Sanders, R.W. (2018). Immunogenicity in rabbits of HIV-1 SOSIP trimers from Clades A, B, and C, given individually, sequentially, or in combination. J. Virol. *92*, e01957-17. https://doi.org/10.1128/JVI.01957-17.
56. Klasse, P.J., LaBranche, C.C., Ketas, T.J., Ozorowski, G., Cupo, A., Pugach, P., Ringe, R.P., Golabek, M., van Gils, M.J., Guttman, M., et al. (2016). Sequential and simultaneous immunization of rabbits with HIV-1 envelope glycoprotein SOSIP.664 trimers from Clades A, B and C. PLoS Pathog. *12*, e1005864. https://doi.org/10.1371/journal.ppat.1005864.
57. Sanders, R.W., van Gils, M.J., Derking, R., Sok, D., Ketas, T.J., Burger, J.A., Ozorowski, G., Cupo, A., Simonich, C., Goo, L., et al. (2015). HIV-1 VACCINES. HIV-1 neutralizing antibodies induced by native-like envelope trimers. Science *349*, aac4223. https://doi.org/10.1126/science.aac4223.
58. de Taeye, S.W., Ozorowski, G., Torrents de la Peña, A., Guttman, M., Julien, J.P., van den Kerkhof, T.L.G.M., Burger, J.A., Pritchard, L.K., Pugach, P., Yasmeen, A., et al. (2015). Immunogenicity of stabilized HIV-1 envelope trimers with reduced exposure of non-neutralizing epitopes. Cell *163*, 1702–1715. https://doi.org/10.1016/j.cell.2015.11.056.
59. Dubrovskaya, V., Tran, K., Ozorowski, G., Guenaga, J., Wilson, R., Bale, S., Cottrell, C.A., Turner, H.L., Seabright, G., O'Dell, S., et al. (2019). Vaccination with glycan-modified HIV NFL envelope trimer-liposomes elicits broadly neutralizing antibodies to multiple sites of vulnerability. Immunity *51*, 915–929.e7. https://doi.org/10.1016/j.immuni.2019.10.008.
60. Pancera, M., Changela, A., and Kwong, P.D. (2017). How HIV-1 entry mechanism and broadly neutralizing antibodies guide structure-based vaccine design. Curr. Opin. HIV AIDS *12*, 229–240. https://doi.org/10.1097/COH.0000000000000360.
61. Wibmer, C.K., Moore, P.L., and Morris, L. (2015). HIV broadly neutralizing antibody targets. Curr. Opin. HIV AIDS *10*, 135–143. https://doi.org/10.1097/COH.0000000000000153.
62. Zhou, T., Lynch, R.M., Chen, L., Acharya, P., Wu, X., Doria-Rose, N.A., Joyce, M.G., Lingwood, D., Soto, C., Bailer, R.T., et al. (2015). Structural repertoire of HIV-1-neutralizing antibodies targeting the CD4 supersite in 14 donors. Cell *161*, 1280–1292. https://doi.org/10.1016/j.cell.2015.05.007.
63. Zhou, T., Xu, L., Dey, B., Hessell, A.J., Van Ryk, D., Xiang, S.H., Yang, X., Zhang, M.Y., Zwick, M.B., Arthos, J., et al. (2007). Structural definition of a conserved neutralization epitope on HIV-1 gp120. Nature *445*, 732–737. https://doi.org/10.1038/nature05580.
64. Zhou, T., Yang, Z., Xu, L., Hessell, A.J., Burton, D.R., Nabel, G.J., and Kwong, P.D. (2009). P04-38. Crystal structure of gp120 in complex with the CD4-binding-site antibody b13 suggests precise targeting is needed for neutralization. Retrovirology *6*, P66. https://doi.org/10.1186/1742-4690-6-S3-P66.
65. Tran, K., Poulsen, C., Guenaga, J., de Val, N., Wilson, R., Sundling, C., Li, Y., Stanfield, R.L., Wilson, I.A., Ward, A.B., et al. (2014). Vaccine-elicited primate antibodies use a distinct approach to the HIV-1 primary receptor binding site informing vaccine redesign. Proc. Natl. Acad. Sci. USA *111*, E738–E747. https://doi.org/10.1073/pnas.1319512111.
66. Andrabi, R., Voss, J.E., Liang, C.H., Briney, B., McCoy, L.E., Wu, C.Y., Wong, C.H., Poignard, P., and Burton, D.R. (2015). Identification of common features in prototype broadly neutralizing antibodies to HIV envelope V2 apex to facilitate vaccine design. Immunity *43*, 959–973. https://doi.org/10.1016/j.immuni.2015.10.014.
67. Pejchal, R., Doores, K.J., Walker, L.M., Khayat, R., Huang, P.S., Wang, S.K., Stanfield, R.L., Julien, J.P., Ramos, A., Crispin, M., et al. (2011). A potent and broad neutralizing antibody recognizes and penetrates the HIV glycan shield. Science *334*, 1097–1103. https://doi.org/10.1126/science.1213256.
68. Julien, J.P., Sok, D., Khayat, R., Lee, J.H., Doores, K.J., Walker, L.M., Ramos, A., Diwanji, D.C., Pejchal, R., Cupo, A., et al. (2013). Broadly neutralizing antibody PGT121 allosterically modulates CD4 binding via recognition of the HIV-1 gp120 V3 base and multiple surrounding glycans. PLoS Pathog. *9*, e1003342. https://doi.org/10.1371/journal.ppat.1003342.
69. Irimia, A., Serra, A.M., Sarkar, A., Jacak, R., Kalyuzhniy, O., Sok, D., Saye-Francisco, K.L., Schiffner, T., Tingle, R., Kubitz, M., et al. (2017). Lipid interactions and angle of approach to the HIV-1 viral membrane of broadly neutralizing antibody 10E8: Insights for vaccine and therapeutic design. PLoS Pathog. *13*, e1006212. https://doi.org/10.1371/journal.ppat.1006212.
70. Kwong, P.D., Doyle, M.L., Casper, D.J., Cicala, C., Leavitt, S.A., Majeed, S., Steenbeke, T.D., Venturi, M., Chaiken, I., Fung, M., et al. (2002). HIV-1 evades antibody-mediated neutralization through conformational masking of receptor-binding sites. Nature *420*, 678–682. https://doi.org/10.1038/nature01188.
71. Haynes, B.F., Wiehe, K., Borrow, P., Saunders, K.O., Korber, B., Wagh, K., McMichael, A.J., Kelsoe, G., Hahn, B.H., Alt, F., and Shaw, G.M. (2023). Strategies for HIV-1 vaccines that induce broadly neutralizing antibodies. Nat. Rev. Immunol. *23*, 142–158. https://doi.org/10.1038/s41577-022-00753-w.
72. Haynes, B.F., Kelsoe, G., Harrison, S.C., and Kepler, T.B. (2012). B-cell-lineage immunogen design in vaccine development with HIV-1 as a case study. Nat. Biotechnol. *30*, 423–433. https://doi.org/10.1038/nbt.2197.
73. Haynes, B.F., and Verkoczy, L. (2014). AIDS/HIV. Host controls of HIV neutralizing antibodies. Science *344*, 588–589. https://doi.org/10.1126/science.1254990.
74. Sok, D., and Burton, D.R. (2018). Recent progress in broadly neutralizing antibodies to HIV. Nat. Immunol. *19*, 1179–1188. https://doi.org/10.1038/s41590-018-0235-7.
75. Kwong, P.D., and Mascola, J.R. (2018). HIV-1 vaccines based on antibody identification, B cell ontogeny, and epitope structure. Immunity *48*, 855–871. https://doi.org/10.1016/j.immuni.2018.04.029.
76. McCoy, L.E., and Burton, D.R. (2017). Identification and specificity of broadly neutralizing antibodies against HIV. Immunol. Rev. *275*, 11–20. https://doi.org/10.1111/imr.12484.
77. Bricault, C.A., Yusim, K., Seaman, M.S., Yoon, H., Theiler, J., Giorgi, E.E., Wagh, K., Theiler, M., Hraber, P., Macke, J.P., et al. (2019). HIV-1 neutralizing antibody signatures and application to epitope-targeted vaccine design. Cell Host Microbe *25*, 59–72.e8. https://doi.org/10.1016/j.chom.2018.12.001.
78. Klein, F., Diskin, R., Scheid, J.F., Gaebler, C., Mouquet, H., Georgiev, I.S., Pancera, M., Zhou, T., Incesu, R.B., Fu, B.Z., et al. (2013). Somatic mutations of the immunoglobulin framework are generally required for broad and potent HIV-1 neutralization. Cell *153*, 126–138. https://doi.org/10.1016/j.cell.2013.03.018.
79. Go, E.P., Ding, H., Zhang, S., Ringe, R.P., Nicely, N., Hua, D., Steinbock, R.T., Golabek, M., Alin, J., Alam, S.M., et al. (2017). Glycosylation benchmark profile for HIV-1 envelope glycoprotein production based on eleven Env trimers. J. Virol. *91*, e02428-16. https://doi.org/10.1128/JVI.02428-16.
80. Cao, L., Pauthner, M., Andrabi, R., Rantalainen, K., Berndsen, Z., Diedrich, J.K., Menis, S., Sok, D., Bastidas, R., Park, S.K.R., et al. (2018). Differential processing of HIV envelope glycans on the virus and soluble recombinant trimer. Nat. Commun. *9*, 3693. https://doi.org/10.1038/s41467-018-06121-4.
81. Torrents de la Peña, A., Rantalainen, K., Cottrell, C.A., Allen, J.D., van Gils, M.J., Torres, J.L., Crispin, M., Sanders, R.W., and Ward, A.B. (2019). Similarities and differences between native HIV-1 envelope glycoprotein trimers and stabilized soluble trimer mimetics. PLoS Pathog. *15*, e1007920. https://doi.org/10.1371/journal.ppat.1007920.
82. Bradley, T., Trama, A., Tumba, N., Gray, E., Lu, X., Madani, N., Jahanbakhsh, F., Eaton, A., Xia, S.M., Parks, R., et al. (2016). Amino acid changes in the HIV-1 gp41 membrane proximal region control virus neutralization sensitivity. EBioMedicine *12*, 196–207. https://doi.org/10.1016/j.ebiom.2016.08.045.
83. Ringe, R., and Bhattacharya, J. (2012). Association of enhanced HIV-1 neutralization by a single Y681H substitution in gp41 with increased gp120-CD4 interaction and macrophage infectivity.

PLoS One *7*, e37157. https://doi.org/10.1371/journal.pone.0037157.
84. Blish, C.A., Nguyen, M.A., and Overbaugh, J. (2008). Enhancing exposure of HIV-1 neutralization epitopes through mutations in gp41. PLoS Med. *5*, e9. https://doi.org/10.1371/journal.pmed.0050009.
85. Lovelace, E., Xu, H., Blish, C.A., Strong, R., and Overbaugh, J. (2011). The role of amino acid changes in the human immunodeficiency virus type 1 transmembrane domain in antibody binding and neutralization. Virology *421*, 235–244. https://doi.org/10.1016/j.virol.2011.09.032.
86. Salimi, H., Johnson, J., Flores, M.G., Zhang, M.S., O'Malley, Y., Houtman, J.C., Schlievert, P.M., and Haim, H. (2020). The lipid membrane of HIV-1 stabilizes the viral envelope glycoproteins and modulates their sensitivity to antibody neutralization. J. Biol. Chem. *295*, 348–362. https://doi.org/10.1074/jbc.RA119.009481.
87. Wang, Q., Esnault, F., Zhao, M., Chiu, T.J., Smith, A.B., III, Nguyen, H.T., and Sodroski, J.G. (2022). Global increases in human immunodeficiency virus neutralization sensitivity due to alterations in the membrane-proximal external region of the envelope glycoprotein can be minimized by distant State 1-stabilizing changes. J. Virol. *96*, e0187821. https://doi.org/10.1128/jvi.01878-21.
88. Zhou, R., Zhang, S., Nguyen, H.T., Ding, H., Gaffney, A., Kappes, J.C., Smith, A.B., III, and Sodroski, J.G. (2023). Conformations of human immunodeficiency virus envelope glycoproteins in detergents and styrene-maleic acid lipid particles. J. Virol. *97*, e0032723. https://doi.org/10.1128/jvi.00327-23.
89. Wang, K., Zhang, S., Go, E.P., Ding, H., Wang, W.L., Nguyen, H.T., Kappes, J.C., Desaire, H., Sodroski, J., and Mao, Y. (2023). Asymmetric conformations of cleaved HIV-1 envelope glycoprotein trimers in styrene-maleic acid lipid nanoparticles. Commun. Biol. *6*, 535. https://doi.org/10.1038/s42003-023-04916-w.
90. Nguyen, H.T., Wang, Q., Anang, S., and Sodroski, J.G. (2023). Characterization of the human immunodeficiency virus (HIV-1) envelope glycoprotein conformational states on infectious virus particles. J. Virol. *97*, e0185722. https://doi.org/10.1128/jvi.01857-22.
91. Kassa, A., Madani, N., Schön, A., Haim, H., Finzi, A., Xiang, S.H., Wang, L., Princiotto, A., Pancera, M., Courter, J., et al. (2009). Transitions to and from the CD4-bound conformation are modulated by a single-residue change in the human immunodeficiency virus type 1 gp120 inner domain. J. Virol. *83*, 8364–8378. https://doi.org/10.1128/JVI.00594-09.
92. Sanders, R.W., Derking, R., Cupo, A., Julien, J.P., Yasmeen, A., de Val, N., Kim, H.J., Blattner, C., de la Peña, A.T., Korzun, J., et al. (2013). A next-generation cleaved, soluble HIV-1 Env trimer, BG505 SOSIP.664 gp140, expresses multiple epitopes for broadly neutralizing but not non-neutralizing antibodies. PLoS Pathog. *9*, e1003618. https://doi.org/10.1371/journal.ppat.1003618.
93. Struwe, W.B., Chertova, E., Allen, J.D., Seabright, G.E., Watanabe, Y., Harvey, D.J., Medina-Ramirez, M., Roser, J.D., Smith, R., Westcott, D., et al. (2018). Site-specific glycosylation of virion-derived HIV-1 Env is mimicked by a soluble trimeric immunogen. Cell Rep. *24*, 1958–1966.e5. https://doi.org/10.1016/j.celrep.2018.07.080.
94. Lu, M., Ma, X., Castillo-Menendez, L.R., Gorman, J., Alsahafi, N., Ermel, U., Terry, D.S., Chambers, M., Peng, D., Zhang, B., et al. (2019). Associating HIV-1 envelope glycoprotein structures with states on the virus observed by smFRET. Nature *568*, 415–419. https://doi.org/10.1038/s41586-019-1101-y.
95. Castillo-Menendez, L.R., Nguyen, H.T., and Sodroski, J. (2019). Conformational differences between functional human immunodeficiency virus envelope glycoprotein trimers and stabilized soluble trimers. J. Virol. *93*, 10–1128. https://doi.org/10.1128/JVI.01709-18.
96. Mangala Prasad, V., Leaman, D.P., Lovendahl, K.N., Croft, J.T., Benhaim, M.A., Hodge, E.A., Zwick, M.B., and Lee, K.K. (2022). Cryo-ET of Env on intact HIV virions reveals structural variation and positioning on the Gag lattice. Cell *185*, 641–653.e17. https://doi.org/10.1016/j.cell.2022.01.013.
97. Tong, T., D'Addabbo, A., Xu, J., Chawla, H., Nguyen, A., Ochoa, P., Crispin, M., and Binley, J.M. (2023). Impact of stabilizing mutations on the antigenic profile and glycosylation of membrane-expressed HIV-1 envelope glycoprotein. PLoS Pathog. *19*, e1011452. https://doi.org/10.1371/journal.ppat.1011452.
98. Torrents de la Peña, A., and Sanders, R.W. (2018). Stabilizing HIV-1 envelope glycoprotein trimers to induce neutralizing antibodies. Retrovirology *15*, 1–11. https://doi.org/10.1186/s12977-018-0445-y.
99. de la Pena, A.T., Julien, J.P., de Taeye, S.W., Garces, F., Guttman, M., Ozorowski, G., Pritchard, L.K., Behrens, A.J., Go, E.P., Burger, J.A., et al. (2017). Improving the immunogenicity of native-like HIV-1 envelope trimers by hyperstabilization. Cell Rep. *20*, 1805–1817. https://doi.org/10.1016/j.celrep.2017.07.077.
100. He, L., Kumar, S., Allen, J.D., Huang, D., Lin, X., Mann, C.J., Saye-Francisco, K.L., Copps, J., Sarkar, A., Blizard, G.S., et al. (2018). HIV-1 vaccine design through minimizing envelope metastability. Sci. Adv. *4*, eaau6769. https://doi.org/10.1126/sciadv.aau6769.
101. Guenaga, J., de Val, N., Tran, K., Feng, Y., Satchwell, K., Ward, A.B., and Wyatt, R.T. (2015). Well-ordered trimeric HIV-1 subtype B and C soluble spike mimetics generated by negative selection display native-like properties. PLoS Pathog. *11*, e1004570. https://doi.org/10.1371/journal.ppat.1004570.
102. Guenaga, J., Dubrovskaya, V., de Val, N., Sharma, S.K., Carrette, B., Ward, A.B., and Wyatt, R.T. (2015). Structure-guided redesign increases the propensity of HIV Env to generate highly stable soluble trimers. J. Virol. *90*, 2806–2817. https://doi.org/10.1128/JVI.02652-15.
103. Georgiev, I.S., Joyce, M.G., Yang, Y., Sastry, M., Zhang, B., Baxa, U., Chen, R.E., Druz, A., Lees, C.R., Narpala, S., et al. (2015). Single-chain soluble BG505.SOSIP gp140 trimers as structural and antigenic mimics of mature closed HIV-1 Env. J. Virol. *89*, 5318–5329. https://doi.org/10.1128/JVI.03451-14.
104. Lu, M., Ma, X., Reichard, N., Terry, D.S., Arthos, J., Smith, A.B., III, Sodroski, J.G., Blanchard, S.C., and Mothes, W. (2020). Shedding-resistant HIV-1 envelope glycoproteins adopt downstream conformations that remain responsive to conformation-preferring ligands. J. Virol. *94*, e00597-20. https://doi.org/10.1128/JVI.00597-20.
105. Nguyen, H.T., Alsahafi, N., Finzi, A., and Sodroski, J.G. (2019). Effects of the SOS (A501C/T605C) and DS (I201C/A433C) Disulfide bonds on HIV-1 membrane envelope glycoprotein conformation and function. J. Virol. *93*, e00304-19. https://doi.org/10.1128/JVI.00304-19.
106. Alsahafi, N., Debbeche, O., Sodroski, J., and Finzi, A. (2015). Effects of the I559P gp41 change on the conformation and function of the human immunodeficiency virus (HIV-1) membrane envelope glycoprotein trimer. PLoS One *10*, e0122111. https://doi.org/10.1371/journal.pone.0122111.
107. Alsahafi, N., Anand, S.P., Castillo-Menendez, L., Verly, M.M., Medjahed, H., Prévost, J., Herschhorn, A., Richard, J., Schön, A., Melillo, B., et al. (2018). SOSIP changes affect human immunodeficiency virus type 1 envelope glycoprotein conformation and CD4 engagement. J. Virol. *92*, e01080-18. https://doi.org/10.1128/JVI.01080-18.
108. Kesavardhana, S., and Varadarajan, R. (2014). Stabilizing the native trimer of HIV-1 Env by destabilizing the heterodimeric interface of the gp41 postfusion six-helix bundle. J. Virol. *88*, 9590–9604. https://doi.org/10.1128/JVI.00494-14.
109. Das, R., Datta, R., and Varadarajan, R. (2020). Probing the structure of the HIV-1 envelope trimer using aspartate scanning mutagenesis. J. Virol. *94*, e01426-20. https://doi.org/10.1128/JVI.01426-20.
110. Zhang, Z., Wang, Q., Nguyen, H.T., Chen, H.-C., Chiu, T.-J., Smith Iii, A.B., and Sodroski, J.G. (2023). Alterations in gp120 glycans or the gp41 fusion peptide-proximal region modulate the stability of the human immunodeficiency virus (HIV-1) envelope glycoprotein pretriggered conformation. J. Virol. *97*, e0059223. https://doi.org/10.1128/JVI.00592-23.
111. Kassa, A., Finzi, A., Pancera, M., Courter, J.R., Smith, A.B., III, and Sodroski, J. (2009). Identification of a human immunodeficiency virus type 1 envelope glycoprotein variant resistant to cold inactivation. J. Virol. *83*, 4476–4488. https://doi.org/10.1128/JVI.02110-08.
112. Chuang, G.Y., Geng, H., Pancera, M., Xu, K., Cheng, C., Acharya, P., Chambers, M., Druz, A., Tsybovsky, Y., Wanninger, T.G., et al. (2017). Structure-based design of a soluble prefusion-closed HIV-1 Env trimer with reduced CD4 affinity and improved immunogenicity. J. Virol. *91*, e02268-16. https://doi.org/10.1128/JVI.02268-16.
113. Leaman, D.P., and Zwick, M.B. (2013). Increased functional stability and homogeneity of viral envelope spikes through directed evolution. PLoS Pathog. *9*, e1003184. https://doi.org/10.1371/journal.ppat.1003184.
114. Gift, S.K., Leaman, D.P., Zhang, L., Kim, A.S., and Zwick, M.B. (2017). Functional stability of HIV-1 envelope trimer affects accessibility to broadly neutralizing antibodies at its apex. J. Virol. *91*, e01216-17. https://doi.org/10.1128/JVI.01216-17.
115. Anang, S., Zhang, S., Fritschi, C., Chiu, T.-J., Yang, D., Smith Iii, A.B., Madani, N., and Sodroski, J. (2023). V3 tip determinants of susceptibility to inhibition by CD4-mimetic

compounds in natural clade A human immunodeficiency virus (HIV-1) envelope glycoproteins. J. Virol. *97*, e0117123. https://doi.org/10.1128/JVI.01171-23.

116. Dorr, P., Westby, M., Dobbs, S., Griffin, P., Irvine, B., Macartney, M., Mori, J., Rickett, G., Smith-Burchnell, C., Napier, C., et al. (2005). Maraviroc (UK-427,857), a potent, orally bioavailable, and selective small-molecule inhibitor of chemokine receptor CCR5 with broad-spectrum anti-human immunodeficiency virus type 1 activity. Antimicrob. Agents Chemother. *49*, 4721–4732. https://doi.org/10.1128/AAC.49.11.4721-4732.2005.
117. Chen, L., Kwon, Y.D., Zhou, T., Wu, X., O'Dell, S., Cavacini, L., Hessell, A.J., Pancera, M., Tang, M., Xu, L., et al. (2009). Structural basis of immune evasion at the site of CD4 attachment on HIV-1 gp120. Science *326*, 1123–1127. https://doi.org/10.1126/science.1175868.
118. Liu, J., Bartesaghi, A., Borgnia, M.J., Sapiro, G., and Subramaniam, S. (2008). Molecular architecture of native HIV-1 gp120 trimers. Nature *455*, 109–113. https://doi.org/10.1038/nature07159.
119. Ozorowski, G., Pallesen, J., de Val, N., Lyumkis, D., Cottrell, C.A., Torres, J.L., Copps, J., Stanfield, R.L., Cupo, A., Pugach, P., et al. (2017). Open and closed structures reveal allostery and pliability in the HIV-1 envelope spike. Nature *547*, 360–363. https://doi.org/10.1038/nature23010.
120. Sattentau, Q.J., and Moore, J.P. (1991). Conformational changes induced in the human immunodeficiency virus envelope glycoprotein by soluble CD4 binding. J. Exp. Med. *174*, 407–415. https://doi.org/10.1084/jem.174.2.407.
121. Sattentau, Q.J., Moore, J.P., Vignaux, F., Traincard, F., and Poignard, P. (1993). Conformational changes induced in the envelope glycoproteins of the human and simian immunodeficiency viruses by soluble receptor binding. J. Virol. *67*, 7383–7393. https://doi.org/10.1128/JVI.67.12.7383-7393.1993.
122. Mbah, H.A., Burda, S., Gorny, M.K., Williams, C., Revesz, K., Zolla-Pazner, S., and Nyambi, P.N. (2001). Effect of soluble CD4 on exposure of epitopes on primary, intact, native human immunodeficiency virus type 1 virions of different genetic clades. J. Virol. *75*, 7785–7788. https://doi.org/10.1128/JVI.75.16.7785-7788.2001.
123. Huang, C.C., Tang, M., Zhang, M.Y., Majeed, S., Montabana, E., Stanfield, R.L., Dimitrov, D.S., Korber, B., Sodroski, J., Wilson, I.A., et al. (2005). Structure of a V3-containing HIV-1 gp120 core. Science *310*, 1025–1028. https://doi.org/10.1126/science.1118398.
124. Chakrabarti, B.K., Walker, L.M., Guenaga, J.F., Ghobbeh, A., Poignard, P., Burton, D.R., and Wyatt, R.T. (2011). Direct antibody access to the HIV-1 membrane-proximal external region positively correlates with neutralization sensitivity. J. Virol. *85*, 8217–8226. https://doi.org/10.1128/JVI.00756-11.
125. Baalwa, J., Wang, S., Parrish, N.F., Decker, J.M., Keele, B.F., Learn, G.H., Yue, L., Ruzagira, E., Ssemwanga, D., Kamali, A., et al. (2013). Molecular identification, cloning and characterization of transmitted/founder HIV-1 subtype A, D and A/D infectious molecular clones. Virology *436*, 33–48. https://doi.org/10.1016/j.virol.2012.10.009.
126. Li, M., Salazar-Gonzalez, J.F., Derdeyn, C.A., Morris, L., Williamson, C., Robinson, J.E., Decker, J.M., Li, Y., Salazar, M.G., Polonis, V.R., et al. (2006). Genetic and neutralization properties of subtype C human immunodeficiency virus type 1 molecular env clones from acute and early heterosexually acquired infections in Southern Africa. J. Virol. *80*, 11776–11790. https://doi.org/10.1128/JVI.01730-06.
127. O'Brien, W.A., Koyanagi, Y., Namazie, A., Zhao, J.Q., Diagne, A., Idler, K., Zack, J.A., and Chen, I.S. (1990). HIV-1 tropism for mononuclear phagocytes can be determined by regions of gp120 outside the CD4-binding domain. Nature *348*, 69–73. https://doi.org/10.1038/348069a0.
128. Walker, L.M., Phogat, S.K., Chan-Hui, P.Y., Wagner, D., Phung, P., Goss, J.L., Wrin, T., Simek, M.D., Fling, S., Mitcham, J.L., et al. (2009). Broad and potent neutralizing antibodies from an African donor reveal a new HIV-1 vaccine target. Science *326*, 285–289. https://doi.org/10.1126/science.1178746.
129. McGee, K., Haim, H., Korioth-Schmitz, B., Espy, N., Javanbakht, H., Letvin, N., and Sodroski, J. (2014). The selection of low envelope glycoprotein reactivity to soluble CD4 and cold during simian-human immunodeficiency virus infection of rhesus macaques. J. Virol. *88*, 21–40. https://doi.org/10.1128/JVI.01558-13.
130. Blattner, C., Lee, J.H., Sliepen, K., Derking, R., Falkowska, E., de la Peña, A.T., Cupo, A., Julien, J.P., van Gils, M., Lee, P.S., et al. (2014). Structural delineation of a quaternary, cleavage-dependent epitope at the gp41-gp120 interface on intact HIV-1 Env trimers. Immunity *40*, 669–680. https://doi.org/10.1016/j.immuni.2014.04.008.
131. Huang, J., Kang, B.H., Pancera, M., Lee, J.H., Tong, T., Feng, Y., Imamichi, H., Georgiev, I.S., Chuang, G.Y., Druz, A., et al. (2014). Broad and potent HIV-1 neutralization by a human antibody that binds the gp41-gp120 interface. Nature *515*, 138–142. https://doi.org/10.1038/nature13601.
132. Moore, J.P., Trkola, A., Korber, B., Boots, L.J., Kessler, J.A., 2nd, McCutchan, F.E., Mascola, J., Ho, D.D., Robinson, J., and Conley, A.J. (1995). A human monoclonal antibody to a complex epitope in the V3 region of gp120 of human immunodeficiency virus type 1 has broad reactivity within and outside clade B. J. Virol. *69*, 122–130. https://doi.org/10.1128/JVI.69.1.122-130.1995.
133. Madani, N., Princiotto, A.M., Easterhoff, D., Bradley, T., Luo, K., Williams, W.B., Liao, H.X., Moody, M.A., Phad, G.E., Vázquez Bernat, N., et al. (2016). Antibodies elicited by multiple envelope glycoprotein immunogens in primates neutralize primary human immunodeficiency viruses (HIV-1) sensitized by CD4-mimetic compounds. J. Virol. *90*, 5031–5046. https://doi.org/10.1128/JVI.03211-15.
134. Byrn, R.A., Mordenti, J., Lucas, C., Smith, D., Marsters, S.A., Johnson, J.S., Cossum, P., Chamow, S.M., Wurm, F.M., Gregory, T., et al. (1990). Biological properties of a CD4 immunoadhesin. Nature *344*, 667–670. https://doi.org/10.1038/344667a0.
135. Mirzabekov, T., Bannert, N., Farzan, M., Hofmann, W., Kolchinsky, P., Wu, L., Wyatt, R., and Sodroski, J. (1999). Enhanced expression, native purification, and characterization of CCR5, a principal HIV-1 coreceptor. J. Biol. Chem. *274*, 28745–28750. https://doi.org/10.1074/jbc.274.40.28745.
136. Holland, A.U., Munk, C., Lucero, G.R., Nguyen, L.D., and Landau, N.R. (2004). Alpha-complementation assay for HIV envelope glycoprotein-mediated fusion. Virology *319*, 343–352. https://doi.org/10.1016/j.virol.2003.11.012.
137. Poznansky, M., Lever, A., Bergeron, L., Haseltine, W., and Sodroski, J. (1991). Gene transfer into human lymphocytes by a defective human immunodeficiency virus Type 1 vector. J. Virol. *65*, 532–536. https://doi.org/10.1128/JVI.65.1.532-536.1991.
138. Parolin, C., Taddeo, B., Palú, G., and Sodroski, J. (1996). Use of cis- and trans-acting viral regulatory sequences to improve expression of human immunodeficiency virus vectors in human lymphocytes. Virology *222*, 415–422. https://doi.org/10.1006/viro.1996.0438.
139. Adachi, A., Gendelman, H.E., Koenig, S., Folks, T., Willey, R., Rabson, A., and Martin, M.A. (1986). Production of acquired immunodeficiency syndrome-associated retrovirus in human and nonhuman cells transfected with an infectious molecular clone. J. Virol. *59*, 284–291. https://doi.org/10.1128/JVI.59.2.284-291.1986.
140. Trkola, A., Purtscher, M., Muster, T., Ballaun, C., Buchacher, A., Sullivan, N., Srinivasan, K., Sodroski, J., Moore, J.P., and Katinger, H. (1996). Human monoclonal antibody 2G12 defines a distinctive neutralization epitope on the gp120 glycoprotein of human immunodeficiency virus type 1. J. Virol. *70*, 1100–1108. https://doi.org/10.1128/JVI.70.2.1100-1108.
141. Walker, L.M., Huber, M., Doores, K.J., Falkowska, E., Pejchal, R., Julien, J.P., Wang, S.K., Ramos, A., Chan-Hui, P.Y., Moyle, M., et al. (2011). Broad neutralization coverage of HIV by multiple highly potent antibodies. Nature *477*, 466–470. https://doi.org/10.1038/nature10373.
142. Caskey, M., Klein, F., Lorenzi, J.C.C., Seaman, M.S., West, A.P., Jr., Buckley, N., Kremer, G., Nogueira, L., Braunschweig, M., Scheid, J.F., et al. (2015). Viraemia suppressed in HIV-1-infected humans by broadly neutralizing antibody 3BNC117. Nature *522*, 487–491. https://doi.org/10.1038/nature14411.
143. Pancera, M., Shahzad-Ul-Hussan, S., Doria-Rose, N.A., McLellan, J.S., Bailer, R.T., Dai, K., Loesgen, S., Louder, M.K., Staupe, R.P., Yang, Y., et al. (2013). Structural basis for diverse N-glycan recognition by HIV-1-neutralizing V1-V2-directed antibody PG16. Nat. Struct. Mol. Biol. *20*, 804–813. https://doi.org/10.1038/nsmb.2600.
144. Muster, T., Steindl, F., Purtscher, M., Trkola, A., Klima, A., Himmler, G., Rüker, F., and Katinger, H. (1993). A conserved neutralizing epitope on gp41 of human immunodeficiency virus type 1. J. Virol. *67*, 6642–6647. https://doi.org/10.1128/JVI.67.11.6642-6647.
145. Sun, Z.Y.J., Oh, K.J., Kim, M., Yu, J., Brusic, V., Song, L., Qiao, Z., Wang, J.H., Wagner, G., and Reinherz, E.L. (2008). HIV-1 broadly neutralizing antibody extracts its epitope from a kinked gp41 ectodomain region on the viral membrane. Immunity *28*, 52–63. https://doi.org/10.1016/j.immuni.2007.11.018.
146. Huang, J., Ofek, G., Laub, L., Louder, M.K., Doria-Rose, N.A., Longo, N.S., Imamichi, H.,

Bailer, R.T., Chakrabarti, B., Sharma, S.K., et al. (2012). Broad and potent neutralization of HIV-1 by a gp41-specific human antibody. Nature *491*, 406–412. https://doi.org/10.1038/nature11544.

147. Posner, M.R., Cavacini, L.A., Emes, C.L., Power, J., and Byrn, R. (1993). Neutralization of HIV-1 by F105, a human monoclonal antibody to the CD4 binding site of gp120. J. Acquir. Immune Defic. Syndr. *6*, 7–14.
148. Conley, A.J., Gorny, M.K., Kessler, J.A., 2nd, Boots, L.J., Ossorio-Castro, M., Koenig, S., Lineberger, D.W., Emini, E.A., Williams, C., and Zolla-Pazner, S. (1994). Neutralization of primary human immunodeficiency virus type 1 isolates by the broadly reactive anti-V3 monoclonal antibody, 447-52D. J. Virol. *68*, 6994–7000. https://doi.org/10.1128/JVI.68.11.6994-7000.1994.
149. Pantophlet, R., Wrin, T., Cavacini, L.A., Robinson, J.E., and Burton, D.R. (2008). Neutralizing activity of antibodies to the V3 loop region of HIV-1 gp120 relative to their epitope fine specificity. Virology *381*, 251–260. https://doi.org/10.1016/j.virol.2008.08.032.
150. Thali, M., Moore, J.P., Furman, C., Charles, M., Ho, D.D., Robinson, J., and Sodroski, J. (1993). Characterization of conserved human immunodeficiency virus type 1 gp120 neutralization epitopes exposed upon gp120-CD4 binding. J. Virol. *67*, 3978–3988. https://doi.org/10.1128/JVI.67.7.3978-3988.1993.
151. Xiang, S.H., Wang, L., Abreu, M., Huang, C.C., Kwong, P.D., Rosenberg, E., Robinson, J.E., and Sodroski, J. (2003). Epitope mapping and characterization of a novel CD4-induced human monoclonal antibody capable of neutralizing primary HIV-1 strains. Virology *315*, 124–134. https://doi.org/10.1016/s0042-6822(03)00521-x.
152. Choe, H., Li, W., Wright, P.L., Vasilieva, N., Venturi, M., Huang, C.C., Grundner, C., Dorfman, T., Zwick, M.B., Wang, L., et al. (2003). Tyrosine sulfation of human antibodies contributes to recognition of the CCR5 binding region of HIV-1 gp120. Cell *114*, 161–170. https://doi.org/10.1016/s0092-8674(03)00508-7.
153. Gohain, N., Tolbert, W.D., Orlandi, C., Richard, J., Ding, S., Chen, X., Bonsor, D.A., Sundberg, E.J., Lu, W., Ray, K., et al. (2016). Molecular basis for epitope recognition by non-neutralizing anti-gp41 antibody F240. Sci. Rep. *6*, 36685. https://doi.org/10.1038/srep36685.
154. Traunecker, A., Schneider, J., Kiefer, H., and Karjalainen, K. (1989). Highly efficient neutralization of HIV with recombinant CD4-immunoglobulin molecules. Nature *339*, 68–70. https://doi.org/10.1038/339068a0.
155. Capon, D.J., Chamow, S.M., Mordenti, J., Marsters, S.A., Gregory, T., Mitsuya, H., Byrn, R.A., Lucas, C., Wurm, F.M., Groopman, J.E., et al. (1989). Designing CD4 immunoadhesins for AIDS therapy. Nature *337*, 525–531. https://doi.org/10.1038/337525a0.
156. Canada-Garcia, D., and Arevalo, J.C. (2023). A simple, reproducible procedure for chemiluminescent Western blot quantification. Bio Protoc *13*, e4667. https://doi.org/10.21769/BioProtoc.4667.

STAR★METHODS

KEY RESOURCES TABLE

REAGENT or RESOURCE	SOURCE	IDENTIFIER
Antibodies		
VRC01	NIH HIV Reagent Program	Cat# ARP-12033 RRID:AB_2491019
VRC03	NIH HIV Reagent Program	Cat# ARP-12032 RRID:AB_2491021
3BNC117	NIH HIV Reagent Program	Cat# ARP-12474 RRID:AB_2491033
PG16	NIH HIV Reagent Program	Cat# ARP-12150 RRID:AB_2491031
PGT145	NIH HIV Reagent Program	Cat# ARP-12703 RRID:AB_2491054
PGT121	Laboratory of Dennis Burton	bNAber ID_24; RRID:AB2491041
PGT151	Laboratory of Dennis Burton; Blattner et al., 2014[130]	N/A
35O22	Laboratory of Mark Connors; Huang et al., 2014[131]	Cat# ARP-12584 and Cat# ARP-12585
b12	NIH HIV Reagent Program	Cat# ARP-2640
2G12	NIH HIV Reagent Program	Cat# ARP-1476 RRID:AB_2819235
2F5	NIH HIV Reagent Program	Cat# ARP-1475 RRID:AB_2491015
4E10	NIH HIV Reagent Program	Cat# ARP-10091 RRID:AB_2491029
10E8.v4	NIH HIV Reagent Program	Cat# ARP-12865 RRID:AB_2491067
19b	Laboratory of James Robinson; Moore et al., 1995[132]	N/A
39F	NIH HIV Reagent Program	Cat# ARP-11437 RRID:AB_2905602
447-52D	NIH HIV Reagent Program	Cat# ARP-4030 RRID:AB_2491016
902090	Laboratory of Barton Haynes; Madani et al., 2016[133]	N/A
F105	NIH HIV Reagent Program	Cat# ARP-857
17b	NIH HIV Reagent Program	Cat# ARP-4091 RRID:AB_2905603
E51	NIH HIV Reagent Program	Cat# ARP-11439
F240	NIH HIV Reagent Program	Cat# ARP-7623
sCD4-Ig	Byrn et al., 1990[134]	Cat# ARP-12960
SIM.2	NIH HIV Reagent Program	Cat# ARP-723
Goat anti-gp120 antibody	Thermo Fisher Scientific	Cat# PA17218
HIV-1 p55 + p24 + p17 antibody	Abcam	Cat#ab63917-100ul
Horseradish peroxidase (HRP)-conjugated rabbit anti-goat IgG	VWR	Cat#RL605-4313

(*Continued on next page*)

Continued

REAGENT or RESOURCE	SOURCE	IDENTIFIER
Peroxidase AffiniPure goat anti-human IgG (H + L) antibody	Jackson ImmunoResearch	Cat#109-035-003; RRID:AB_2337577
HRP-conjugated goat anti-mouse IgG	Jackson ImmunoResearch	Cat#115-035-008; RRID:AB_2313585
HRP-conjugated goat anti-rabbit IgG	Cytiva	Cat#NA934-1ML; RRID:AB_2722659
Bacterial and virus strains		
pNL4-3.AD8	Nguyen et al., 2023[90]	N/A
pNL4-3.JR-FL	Nguyen et al., 2023[90]	N/A
One Shot Stbl3 Chemically Competent E. coli	Life Technologies	Cat#C737303
One Shot TOP10 Chemically Competent E. coli	Life Technologies	Cat#C404003
XL10-Gold Ultracompetent Cells	Agilent	Cat# 200315
Chemicals, peptides, and recombinant proteins		
BNM-III-170	Laboratory of Amos B. Smith III[26]	N/A
CJF-III-288	Laboratory of Amos B. Smith III[27]	N/A
Maraviroc	Selleck Chem	Cat#11580
Luciferase substrate	Promega	Cat#E4550 RRID:AB_1660600
Galacto-Star™ substrate	Thermo Fisher Scientific	Cat#T2255
Protease Inhibitor Cocktail	Roche Diagnostic GmbH	Cat#11836170001
Protein A-agarose	Cytiva	Cat#17078001
Ni-NTA Agarose	QIAGEN	Cat#30230
PNGase F	NEB	Cat#P0704L
Galanthus Nivalis lectin (GNL)-beads	Vector Laboratories	Cat#AL-1243
Lipofectamine 3000	Thermo Fisher Scientific	Cat#100022052
Polyethyleneimine (PEI)	Thermo Fisher Scientific	Cat#043896.01
NuPage LDS sample buffer	Life Technologies	Cat#NP0008
Experimental models: Cell lines		
HEK293T	ATCC	CRL-3216 RRID:CVCL_0063
COS-1	ATCC	CRL-1650 RRID:CVCL_0223
HOS	ATCC	CRL-1543 RRID:CVCL_0312
TZM-bl	NIH HIV Reagent Program	Cat#ARP-8129 RRID:CVCL_B478
Cf2Th-CD4/CCR5	Mirzabekov et al., 1999[135]	N/A
Cf2Th-CCR5	Mirzabekov et al., 1999[135]; NIH HIV Reagent Program	Cat#ARP-4662
Recombinant DNA		
pSVIII env.AD8	Nguyen et al., 2022[32]	N/A
pSVIII env.AD8 mutants	This paper	N/A
pcDNA3.1 Du422.1	Li et al., 2006[126]	N/A
pcDNA3.1 Du422.1 mutants	This paper	N/A
pcDNA3.1 191859	Baalwa et al., 2013[125]	N/A
pcDNA3.1 191859 mutants	This paper	N/A
α-gal expressor plasmid	Holland et al., 2004[136]	N/A
ω-gal expressor plasmid	Holland et al., 2004[136]	N/A

(*Continued on next page*)

Continued

REAGENT or RESOURCE	SOURCE	IDENTIFIER
pNL4-3.Luc R^-E^-	NIH HIV Reagent Program	Cat#ARP-3418
pCMV ΔP1Δenv	Poznansky et al., 1991[137]	N/A
HIV-1.Luc	Parolin et al., 1996[138]	N/A
Software and algorithms		
GraphPad Prism 9	GraphPad Software Inc	https://www.graphpad.com/scientific-software/prism/
ImageJ	The National Institutes of Health	https://imagej.nih.gov/ij/
Bio-Rad Image Lab	Bio-Rad	https://www.bio-rad.com/en-us/product/image-lab-software?ID=KRE6P5E8Z

RESOURCE AVAILABILITY

Lead contact

Requests for further information or reagents and resources should be directed to and will be fulfilled by the lead contact, Joseph Sodroski (joseph_sodroski@dfci.harvard.edu).

Materials availability

Plasmids encoding the wild-type and mutant HIV-1 Envs described in this study are available from the lead contact upon completion of a Materials Transfer Agreement.

Data and code availability

Data: The data reported in this manuscript will be shared by the lead contact upon request after publication.

Code: Not applicable.

Other: Not applicable.

METHOD DETAILS

HIV-1 Env mutants

The wild-type HIV-1_{AD8} *env* cloned in the pSVIIIenv expression plasmid was used as a template to construct HIV-1_{AD8} Env mutants in this study. The signal peptide/N-terminus (residues 1–33) and the cytoplasmic tail C-terminus (residues 751–856) of this Env are derived from the HIV-1_{HXBc2} Env.[32,87,90] "Tri" indicates the Q114E/Q567K/A582T changes,[32] and "FPPR" indicates the presence of Val 532, Met 535 and Gln 543.[110] Changes were introduced by using the QuikChange Lightning site-directed mutagenesis kit (Agilent Technologies). All the HIV-1_{AD8} Env variants contain a His_6 tag at the carboxyl terminus.

The Env variants from the clade C HIV-$1_{Du422.1}$ strain[126] (GenBank DQ411854) and the clade D HIV-1_{191859} strain[125] (GenBank JX236672) were expressed from pcDNA3.1 plasmids. The pcDNA3.1 plasmids expressing the wild-type Env were obtained from George Shaw and Beatrice Hahn (University of Pennsylvania) through the NIH HIV Reagent Program. Mutations were introduced into the *env* genes using a Q5 site-directed mutagenesis kit (New England BioLabs). The presence of the desired mutations was confirmed by DNA sequencing.

A subset of the Env variants was expressed from *env* genes cloned into an infectious HIV-1 provirus in the pNL4-3 plasmid.[139] For the HIV-1_{AD8} Env mutants expressed by proviruses, site-directed changes were introduced into the previously described pNL4-3.AD8 Bam plasmid[90]; these AD8 Envs contain "Bam" changes (S752F/I756F) that decrease viral protease clipping of the gp41 cytoplasmic tail in virus particles.[90] HIV-1_{JR-FL} Env variants were expressed by the pNL4-3.JR-FL E168K plasmid[90]; the E168K change in these Envs allows recognition by V2 quaternary bNAbs.[128] Envs designated "Tri" or "FPPR" contain the changes described above. Env changes in the pNL4-3.AD8 Bam and pNL4-3.JR-FL E168K plasmids were introduced by site-directed mutagenesis using the Q5 polymerase (New England BioLabs). The mutated plasmids were transformed into One Shot Stbl3 chemically competent E.coli (Life Technologies) following the manufacturer's protocol. All mutations were confirmed by DNA sequencing.

Antibodies, sCD4-Ig and small-molecule HIV-1 entry inhibitors

Poorly neutralizing antibodies (F105, 19b, 39F, 447-52D, 902090, 17b, E51 and F240) and broadly neutralizing antibodies (VRC01, VRC03, 3BNC117, b12, PGT145, PG16, PGT151, 35O22, PGT121, 2G12, 2F5, 4E10 and 10E8.v4) against the HIV-1 Env were obtained through the NIH HIV Reagent Program, Division of AIDS, NIAID, NIH. These antibodies were kindly contributed by John C. Kappes (University of Alabama at Birmingham), Dennis Burton (Scripps), Peter Kwong and John Mascola (Vaccine Research Center NIH), Mark Connors (National Institute of Allergy and Infectious Diseases, NIH), Barton Haynes (Duke University), Hermann Katinger (Polymun), James Robinson (Tulane University), Michel Nussenzweig (Rockefeller University) and Marshall Posner (Mount Sinai Medical Center). The SIM.2 anti-CD4 antibody (ARP-723) was obtained from the NIH HIV Reagent Program and was contributed by James Hildreth (Meharry Medical College). The bNAbs include

2G12 against gp120 outer-domain glycans[140]; PGT121 against V3 glycans[141]; VRC03, VRC01, 3BNC117 and b12 against the gp120 CD4-binding site (CD4BS)[62–64,142]; PG16 and PGT145 against quaternary V2 epitopes at the Env trimer apex[128,141,143]; PGT151 and 35O22 against the gp120-gp41 interface[130,131]; and 2F5, 4E10 and 10E8.v4 against the gp41 membrane-proximal external region (MPER).[69,144–146] The pNAbs include F105 against the gp120 CD4BS[147]; 19b, 39F and 447-52D against the gp120 V3 region[132,148,149]; 902090 against the gp120 V2 region[133]; 17b and E51 against gp120 CD4i epitopes[150–152]; and F240 against a Cluster I epitope on gp41.[153]

In sCD4-Ig, the N-terminal two domains of CD4 are fused with the Fc portion of an antibody.[134,154,155]

The CD4-mimetic compounds BNM-III-170 and CJF-III-288 were synthesized as previously described.[26,27] Maraviroc was purchased from Selleckchem. The compounds were dissolved in dimethyl sulfoxide (DMSO) at a stock concentration of 10 mM and diluted to the appropriate concentration in cell culture medium.

Cell lines

HEK293T, TZM-bl and HOS cells (ATCC) were cultured in Dulbecco modified Eagle medium (DMEM) supplemented with 10% fetal bovine serum (FBS) and 100 μg/mL penicillin-streptomycin. Cf2Th-CD4/CCR5 and Cf2Th-CCR5 cells[135] were cultured in the same medium supplemented with 400 μg/mL G418/200 μg/mL hygromycin or 400 μg/mL G418, respectively. All cell culture reagents were from Life Technologies.

Env expression

To evaluate Env processing, subunit association and gp120-trimer association, 3×10^5 HOS cells were seeded in 6-well plates. After 24 h of incubation, they were transfected with pSVIIIenv plasmids encoding His_6-tagged HIV-1_{AD8} Env variants (or pcDNA3.1 plasmids encoding HIV-$1_{Du422.1}$ or HIV-1_{191859} Env variants), using the Lipofectamine 3000 transfection reagent (Thermo Fisher Scientific) according to the manufacturer's instructions. The pSVIIIenv plasmids expressing the HIV-1_{AD8} Env variants were cotransfected with a Tat-expressing plasmid at an 8:1 ratio. Seventy-two hours after transfection, the supernatants were collected and incubated with Galanthus Nivalis Lectin (GNL)-agarose beads (Vector Laboratories) for 1.5 h at room temperature. Beads were washed three times with 1× phosphate-buffered saline (PBS) containing 0.1% NP-40 and processed for western blotting with a goat anti-gp120 antibody (Thermo Fisher Scientific). The cells were lysed in PBS buffer containing 1.0% NP-40 and protease inhibitor (Roche Diagnostic). For HIV-1_{AD8} Env variants, clarified cell lysates were harvested and separated into two portions. One portion was used for the "Input" sample. The other was incubated with Ni-NTA beads at room temperature for 1.5 h. Then the beads were washed, boiled, and the Env proteins analyzed by western blotting. For the HIV-$1_{Du422.1}$ and HIV-1_{191859} Env variants, the cell lysates were clarified and analyzed by western blotting. Western blots were developed with 1:2,500 goat anti-gp120 antibody (Thermo Fisher Scientific) and 1:2,500 HRP-conjugated rabbit anti-goat antibody (VWR). The intensities of the gp120 and gp160 bands from unsaturated western blots were quantified using ImageJ software.[156] The Env processing index was calculated by dividing gp120 by gp160 in the Input/cell lysate samples. The subunit association index was calculated by dividing gp120 in the Input/cell lysate samples by the gp120 in the GNL precipitates. For the HIV-1_{AD8} Env variants, the gp120-trimer association index was calculated by dividing the gp120:gp160 ratio in the Ni-NTA precipitates by the gp120:gp160 ratio in the Input samples. The processing and subunit association indices (and, for the HIV-1_{AD8} Env variants, the gp120-trimer association indices) of the Env mutants were normalized to those of the corresponding wt HIV-1 Env.

Cell-cell fusion assay

For the alpha-complementation assay measuring cell-cell fusion,[136] 2×10^4 COS-1 effector cells were seeded in black-and-white 96-well plates and then cotransfected with plasmids expressing α-gal, Env variants and Tat at a 1:1:0.125 ratio, using Lipofectamine 3000 transfection reagent (Thermo Fisher Scientific) following the manufacturer's protocol. At the same time, Cf2Th-CD4/CCR5 cells target cells in 6-well plates were cotransfected with a plasmid expressing ω-gal using Lipofectamine 3000 transfection reagent. Forty-eight hours after transfection, target cells were detached and resuspended in medium. Medium was aspirated from the effector cells, and target cell suspensions in 50-μL volumes were added to the effector cells (one target-cell well provides sufficient cells for 50 effector-cell wells). Plates were spun at 500 × g for 3 min and then incubated at 37°C in 5% CO_2 for 8 h. Medium was removed, and cells were lysed in Tropix lysis buffer (Thermo Fisher Scientific). The β-galactosidase activity in the cell lysates was measured using the Galacto-Star Reaction Buffer Diluent with Galacto-Star Substrate (Thermo Fisher Scientific), according to the manufacturer's instructions.

Virus infectivity

To produce pseudoviruses, HEK293T cells were cotransfected either with: 1) the Env-expressing pSVIIIenv plasmid, a Tat-encoding plasmid and the luciferase-encoding pNL4-3.Luc.R-E- vector (NIH HIV Reagent Program) at a 1:1:3 μg DNA ratio; or 2) pSVIIIenv or pcDNA3.1 plasmids expressing Env, the pCMVΔP1Δenv HIV-1 Gag-Pol packaging construct,[137] and the firefly luciferase-expressing HIV-1 vector[138] at a 1:1:3 μg DNA ratio using polyethylenimine transfection reagent (Thermo Fisher Scientific). The medium was replaced 6 to 8 h after transfection. The cell supernatants containing pseudoviruses were harvested 72 h later and centrifuged (3500 rpm for 5 min), aliquoted, and either used directly to measure pseudovirus infectivity or stored at −80°C until use.

To compare the infectivity of the variants, pseudoviruses freshly prepared by procedures 1 and 2 were serially diluted in 96-well plates and incubated either with TZM-bl cells in the presence of 20 μg/mL DEAE-dextran or with Cf2Th-CD4/CCR5 cells, respectively. After 48 h of incubation, cells were lysed and the luciferase activity was measured using a luminometer.

Kinetics of cell-cell fusion and virus entry

The cell-cell fusion assay described above was used to estimate the relative rates of cell-cell fusion mediated by the Env variants. Effector cells expressing α-gal, Env and Tat were incubated with Cf2Th-CD4/CCR5 cells expressing ω-gal at 37°C in 5% CO_2 for various lengths of time. The β-galactosidase activity in the cell lysates was measured as described above.

The relative rates of virus entry mediated by the different Envs were estimated using a variation of procedure 1 of the virus infectivity assay described above. Recombinant viruses were produced by transfection of HEK293T cells with pSVIIIenv, pNL4-3.Luc.R-E- and a Tat-expressing plasmid. The virus suspensions were chilled briefly on ice and added to TZM-bl cells. The virus-cell mixtures were centrifuged at 1800 x g for 30 min at 4°C. The medium was removed and replaced with fresh medium warmed to 37°C. The cells were incubated at 37°C in 5% CO_2. At various times, 30 μg/mL 10E8.v4 antibody was added to the medium. Forty-eight hours after beginning the 37°C incubation, the cells were lysed and luciferase activity was measured. Residual virus entry was calculated as the percentage of infection observed when the 10E8.v4 antibody was added at a given time point relative to the level of infection observed in the absence of the 10E8.v4 antibody.

Activation of virus infection by CD4mcs

Recombinant luciferase-expressing viruses pseudotyped with Env variants were incubated with CD4-negative, CCR5-expressing Cf2Th-CCR5 cells in 96-well plates. The plates were centrifuged at 600 x g for 30 min at room temperature. Medium containing serial dilutions of CJF-III-288 was then added. Forty-eight hours later, the cells were lysed and luciferase activity was measured.

Virus sensitivity to cold inactivation

To evaluate virus sensitivity to cold inactivation, pseudoviruses were incubated on ice (at 0°C) for different lengths of time and virus infectivity was subsequently measured on Cf2Th-CD4/CCR5 or TZM-bl cells, as described above.

Virus inhibition/neutralization

The inhibitors to be tested (antibodies, sCD4-Ig, CD4mcs or Maraviroc) were serially diluted in triplicate wells of 96-well plates. Then approximately 100–200 $TCID_{50}$ (50% tissue culture infectious doses) of pseudoviruses was added and incubated at 37°C for 1 h. Subsequently, approximately 2 × 10^4 TZM-bl cells (with 20 μg/mL DEAE-dextran in the medium) or Cf2Th-CD4/CCR5 cells were added to each well and the mixture was incubated at 37°C/5%CO_2 for 48 h. Then the luciferase activity in the cells was measured, as described above. The concentrations of antibodies and other Env ligands that inhibit 50% of infection (the IC_{50} values) were determined by fitting the data in four-parameter dose-response curves using GraphPad Prism 9.

In an assay designed to evaluate the ability of an antibody to neutralize viruses before they engage the target cell, recombinant viruses pseudotyped with Env variants were incubated for 1 h at 37°C with the following concentrations of antibodies: VRC01 (10 μg/mL), 2F5 and 4E10 (20 μg/mL), and 19b, 39F and 447-52D (50 μg/mL). The viruses were then pelleted and the antibody-containing supernatants removed. The virus pellet was resuspended in antibody-free medium and incubated with TZM-bl cells. Forty-eight hours later, luciferase activity was measured.

In an assay designed to measure the ability of antibodies to neutralize virus after virus-cell interaction, recombinant viruses pseudotyped with the Env variants were added to TZM-bl cells. The virus-cell mixtures were centrifuged at 1800 × g for 30 min at room temperature. The medium was removed and replaced with fresh medium containing the antibody. The concentrations of the antibodies were the same as those used in the virus neutralization assay above. Forty-eight hours later, luciferase activity in the TZM-bl cells was measured.

Virus sensitivity to combined exposure to a CD4mc and 0°C

To evaluate the sensitivity of viruses to inhibition by a combined exposure to a CD4mc and cold, pseudoviruses were incubated with either 100 μM BNM-III-170 or 10 μM CJF-III-288 or, as a control, the equivalent concentration of DMSO for 1 h at 37°C. The virus preparations were then incubated on ice for varying lengths of time (up to 19 days). The infectivity of the pseudovirus preparations for TZM-bl or Cf2Th-CD4/CCR5 cells was measured as described above. The half-life of virus infectivity relative to the infectivity of the DMSO-treated virus at day 0 was calculated by fitting the data to a one-phase exponential decay model with GraphPad Prism 9.

Analysis of Env on infectious virus particles produced from proviral clones

To produce virus particles, HEK293T cells were transfected with pNL4-3.env plasmids using polyethyleneimine (Thermo Fisher Scientific). The medium was replaced 4 h after transfection and the cells were incubated at 37°C in 5% CO_2. Seventy-two hours after transfection, the cells were lysed and the supernatants were collected, filtered (0.45 μm) and centrifuged at 14,000 × g or 100,000 × g for 1 h at 4°C to concentrate the virus particles. The pelleted virus particles were resuspended in 1× PBS.

To evaluate Env expression and incorporation into virus particles, clarified cell lysates and the virus particle suspensions were analyzed by western blotting using a nitrocellulose membrane and wet transfer (350 A, 75 min, Bio-Rad). Western blots were incubated with 1:2,000 goat anti-gp120 polyclonal antibody (Invitrogen), 1:2,000 4E10 anti-gp41 antibody, 1:1,000 mouse anti-p24 serum (John C. Kappes, University of Alabama at Birmingham) and 1:10,000 rabbit anti-hsp70 (K-20) antibody (Santa Cruz Biotechnology). The respective HRP-conjugated secondary antibodies were 1:2,000 rabbit anti-goat (VWR), 1:2,000 goat anti-human (Jackson ImmunoResearch), 1:1,000 goat anti-mouse (Jackson ImmunoResearch) and 1:10,000 goat anti-rabbit (Cytiva).

Shedding of gp120 from virus particles

Virus particles resuspended in 1× PBS were divided into 50-μL aliquots and incubated with serial dilutions of the CD4mc BNM-III-170 for 1 h at room temperature or on ice for 1–2 days. Next, 200 μL 1× PBS was added and the samples were centrifuged at 14,000 × g for 1 h at 4°C. Then 220 μL of the supernatants was collected and rotated during incubation with Galanthus Nivalis Lectin (GNL)-agarose beads (Vector Laboratories) for 2 h at room temperature. Beads were washed three times with 1× PBS/0.1% NP-40 and processed for western blotting with a goat anti-gp120 antibody. An aliquot of the virus particle suspension prior to incubation with BNM-III-170 was used as the "Input" sample.

Antigenicity of Env on virus particles

Fifty-μL aliquots of virus particle suspensions in 1× PBS were incubated with a panel of antibodies at 10 μg/mL concentration for 1 h at room temperature. One mL of chilled 1× PBS was added and samples were centrifuged at 14,000 × g for 1 h at 4°C. The pellets were lysed in 100 μL chilled 1× PBS/0.5% NP-40/protease inhibitor cocktail. Lysates were rotated during incubation with Protein A-agarose beads for 1 h at 4°C and washed with chilled 1× PBS/0.1% NP-40 three times. The beads were resuspended in 1× PBS containing NuPage LDS Sample Buffer (Life Technologies) and dithiothreitol (DTT) and used for western blotting, as described above. To prepare the Input (50%) sample, half of the virus particle suspension was mixed with 1 mL chilled 1× PBS and centrifuged at 14,000 × g for 1 h at 4°C; the pellet was resuspended in 1× PBS/LDS/DTT.

To deglycosylate immunoprecipitated complexes, after the Protein A-agarose incubation and washing step, the virus-antibody-Protein A-agarose complexes were boiled in denaturing buffer (New England BioLabs) for 10 min and treated with PNGase F (New England BioLabs) for 1.5 h at 37°C according to the manufacturer's protocol. To prepare the deglycosylated Input (50%), 25 μL of the virus particle suspension was mixed with 1 mL chilled 1× PBS and centrifuged at 14,000 × g for 1 h at 4°C; the pellet was lysed in 1× PBS/0.5% NP-40/protease inhibitor cocktail. The lysate was denatured and PNGase F-treated as described above. The treated proteins were then analyzed by reducing SDS-PAGE and western blotting.

The intensity of protein bands on nonsaturated Western blots was quantified using the Bio-Rad Image Lab program. Statistical significance was evaluated by a two-tailed Student's t test.

QUANTIFICATION AND STATISTICAL ANALYSIS

For virus inhibition assays, the IC_{50} values were determined by fitting the data in 4-parameter dose-response curves using GraphPad Prism 9.

The half-lives of infectivity after virus exposure to cold or cold + CD4mc were calculated by fitting the data to a one-phase exponential decay model with GraphPad Prism 9.

The intensity of protein bands on nonsaturated western blots was quantified using Bio-Rad Image Lab. Statistical significance was evaluated by a two-tailed Student's t test.

Correlations among Env phenotypes were evaluated by Spearman rank order correlation analysis.

Assessment of statistical significance was based on two-tailed *p* values less than 0.05.

The details of quantification and statistical analysis can be found in method details and figure legends.